Spread of a single superclone drives insecticide resistance in *Acyrthosiphon kondoi* across an invasive range

Joshua A. Thia[1,*], Benjamin J. Hunt, Shuchao Wang[2], Bartlomiej J Troczka[2], Courtney J. Brown[1], Leonhard S. Arinanto[1], Evatt Chirgwin[3], Monica Stelmach[1], Kelly Richardson[1], Chinmayee Joglekar[1], Ashritha P. S. Dorai[1], Qiong Yang[1], Marielle Babineau[3], Chris Bass[2], Ary A. Hoffmann[1], Paul A. Umina[1,3]

[1] School of BioSciences, The University of Melbourne, Melbourne, Victoria, Australia

[2] Centre for Ecology and Conservation, University of Exeter, Penryn, Cornwall, UK

[3] Cesar Australia, Brunswick, Victoria, Australia

Name	**ORCID**
Joshua A Thia	https://orcid.org/0000-0001-9084-0959
Benjamin J Hunt	https://orcid.org/0000-0003-3825-9723
Shuchao Wang	https://orcid.org/0009-0003-1025-9155
Bartlomiej J Troczka	https://orcid.org/0000-0001-9177-2441
Courtney J Brown	https://orcid.org/0000-0003-1515-1947
Leonhard S Arinanto	

Evatt Chirgwin	https://orcid.org/0000-0002-8242-3837
Monica Stelmach	https://orcid.org/0009-0006-7671-1775
Kelly Richardson	https://orcid.org/0000-0001-7186-1260
Chinmayee Joglekar	https://orcid.org/0009-0001-5345-9128
Ashritha PS Dorai	https://orcid.org/0009-0004-2928-039X
Qiong Yang	https://orcid.org/0000-0003-3336-5703
Marielle Babineau	https://orcid.org/0009-0008-9524-7765
Chris Bass	https://orcid.org/0000-0002-2590-1492
Ary A Hoffmann	https://orcid.org/0000-0001-9497-7645
Paul A Umina	https://orcid.org/0000-0002-1835-3571

ABSTRACT

Populations under similar selection pressures may adapt via parallel evolution or dispersal of advantageous alleles. Here, we investigated insecticide resistance in the invasive blue-green aphid, *Acyrthosiphon kondoi*, which reproduces clonally in Australia and has rapidly developed resistance across geographic locations. Using genomic, transcriptomic, and experimental approaches, we explored the evolutionary origins and molecular mechanisms of resistance. We developed the first reference genome for *A. kondoi* (443.8 Mb, 28,405 annotated genes, BUSCO score 97.5%) and established isofemale strains from southern Australia with varying resistance statuses. All resistant strains shared a common ancestor, supporting the spread of a resistant 'superclone' distinct from susceptible strains. Resistance was associated with overexpression of an esterase gene homologous to the E4/FE4 esterases linked to multi-chemical resistance in other aphid pests. Functional experiments in *Drosophila melanogaster* confirmed the causal role of this E4-like esterase in resistance to organophosphates, carbamates, and pyrethroids. These findings highlight how clonal dispersal and insecticide overuse can transform local adaptation into a widespread pest management issue. Our results suggest a parallel macroevolutionary response to insecticide selection in *A. kondoi* and other aphid species at the gene family level, but with a distinct regulatory mechanism in *A. kondoi*. Given the rapid spread of the resistant superclone, alternative management strategies, including expanded chemical control options and enhanced biological control, are urgently needed to mitigate this growing pest problem.

INTRODUCTION

Understanding variation in the rise and spread of adaptive traits and their underlying genes is a key issue in evolutionary biology (Cohan and Hoffmann 1989; Korona et al. 1994; Colosimo et al. 2005). When populations or species are exposed to similar selective pressures, they may evolve through parallel changes, reflecting multiple independent evolutionary events. Parallelism might occur only at the phenotypic level (Roda et al. 2013; Magalhaes et al. 2020; Yang et al. 2020; Sprengelmeyer and Pool 2021), or it may extend to the genotypic level, where the same allelic changes are involved. The latter is more likely if populations share standing genetic variation (Colosimo et al. 2005; Magalhaes et al. 2020; Montejo-Kovacevich et al. 2022). Apparent parallel evolution can also arise if gene flow spreads adaptive alleles across areas with similar selective pressures (Endersby-Harshman et al. 2020; Tepolt et al. 2021; Zhang et al. 2023). Indeed, gene flow can assist adaptation to new environmental stressors by introducing adaptive variation into local populations (Chevillon et al. 1999; Bontrager and Angert 2019). Disentangling these processes sheds light on the repeatability of evolution and the origins of adaptive variation in local populations.

Clonal organisms are often considered to have lower adaptive capacity because they lack recombination to produce adaptive gene combinations (Muller 1932; Barraclough et al. 2003). However, when clonal diversity arises from mutation accumulation or rare sexual reproduction, it is possible for selection to drive clonal lineages with adaptive alleles to high frequency, often at the expense of other lineages (Muller 1932; Gerrish and Lenski 1998; Barraclough et al. 2003). Clonal

organisms therefore provide a unique context for tracking the origin and trajectory of adaptive traits and alleles, as these are directly linked to specific (clonal) genetic backgrounds. For example, in the cystic fibrosis-associated bacterium *Pseudomonas aeruginosa*, recurrent selective sweeps have been associated with parallel genetic, transcriptional, and phenotypic changes for adaptive pathogenicity among clonal lineages (Huse et al. 2010; Feliziani et al. 2014; Caballero et al. 2015). In the parasitic protozoan *Toxoplasma gondii*, dominance of three clonal lineages in North American and Europe has been attributed to strong selection on key virulence alleles associated with each of these lineages (Howe and Sibley 1995; Khan et al. 2009). Studies on *Daphnia* species have also shown clear, predictable patterns of changes in clonal frequencies due to variation in competitive abilities of clonal lineages under different environmental conditions (Korpelainen 1986; Steiner et al. 2016; Lyberger and Schoener 2023). And in yeast, tracking of clonal lineages has illustrated how the accumulation of beneficial mutations within clones leads to the dominance of highly fit genotypes (Nguyen Ba et al. 2019).

Insecticide usage in agriculture provides an interesting context for studying adaptation to similar selective environments. Pest species are often exposed to the same insecticide across different populations as part of chemical control strategies (Walsh et al. 2018; Endersby-Harshman et al. 2020; Singh et al. 2021; Thia, Korhonen, et al. 2023). Because insecticides exert their toxicity through very specific protein targets and molecular interactions, there is strong precedence for joint phenotypic and genotypic parallelism in insecticide resistance traits. This has been demonstrated repeatedly, leading to parallel and convergent evolution of the same mutations in

these target proteins that prevent insecticide inhibition – so called 'target-site mutations' (Fournier 2005; Davies et al. 2007). Such parallelism can occur both at the microevolutionary scale among populations (Walsh et al. 2018; Thia, Korhonen, et al. 2023), and at the macroevolutionary scale, leading to convergence among species (Feyereisen et al. 2015). However, alternate mechanisms might also evolve, such as shifts in the expression or efficacy of detoxification proteins, and polygenic resistance can lead to non-parallel genetic mechanisms of insecticide resistance among populations (Field and Devonshire 1998; Crossley et al. 2017; Yang et al. 2020; Thia, Korhonen, et al. 2023).

Although clonal reproduction is uncommon in animal populations, it tends to occur at a relatively higher frequency among invertebrates in agricultural environments (Hoffmann et al. 2008). Aphids (Order: Hemiptera) are a major agricultural arthropod pest: they are sap-sucking insects that damage plant through direct feeding and virus transmission (Blackman and Eastop 2017). Aphid populations are often composed of holocyclic (sexual or asexual, host-alternating) clones, particularly in temperate regions with cold winter temperatures, but they often become anholocyclic (asexual, nonhost-alternating) in more benign climates (Rispe et al. 1998; Rispe and Pierre 1998; Williams and Dixon 2017). Clonal reproduction can dramatically shape the evolutionary trajectory of aphid populations by favouring the dominance of 'superclones'. These are clonal lineages that have acquired highly advantageous traits (through genetic mutation or endosymbiont acquisition) that allow them to spread across broad geographic extents (Gilabert et al. 2015; Godefroid et al. 2024; Mahieu et al. 2024). For agriculturally important aphid species,

insecticide selection can facilitate the spread of superclones carrying insecticide resistance mutations. For example, in the peach potato aphid, *Myzus persicae*, although different genetic lineages carrying resistance have evolved around the world (Singh et al. 2021), there can be significant local sweeps of specific superclones, such as in Australia (Umina et al. 2014; de Little et al. 2017; Ward et al. 2024). Similarly, in the wheat aphid *Sitobion avenae*, a single insecticide resistant clonal lineage has become dominant in the UK, reducing local clonal diversity (Morales-Hojas et al. 2020).

In this study, we investigated the recently evolved insecticide resistance in the blue green aphid, *Acyrthosiphon kondoi*, in its invasive Australian range. This aphid is native to Asia but has become an agricultural pest across the world, including the USA, South America, Africa, and Australia (Ryalls et al. 2013). It is a pest of alfalfa and leguminous grains crops including lentils and lupins (Humphries et al. 2012; Ryalls et al. 2013). In Australia, and in other parts of its invasive range, *A. kondoi* reproduction is mostly asexual (Ryalls et al. 2013), with sexual reproduction often occuring in its native range, though data are limited (Kawada 1992). Historically, there have been scant reports of insecticide resistance in *A. kondoi*. One of the only cases is described in unpublished work from the USA (Natwick et al. 2014). Since then, there have been no documented cases globally for *A. kondoi* until the recent discovery of organophosphate, carbamate, and pyrethroid resistance in Australian populations in 2020 (Chirgwin et al. 2023). This has led to control failures and subsequent economic damage to Australian alfalfa growers (Chirgwin et al. 2023). Outstanding questions

from this work include the evolutionary origins of resistance and the underlying genes contributing to this adaptive trait.

Here, we use the evolved resistance in Australian *A. kondoi* to study the evolutionary origins of apparent parallel adaptation and its genetic basis. We began with a genomics approach to address two initial objectives: (1) to determine whether resistant strains were of the same or different clonal background; and (2) to identify putative genes that might underpin resistance. Our finding of a candidate detoxification gene, an E4-like esterase, led us to address two additional objectives: (3) to validate the differential expression patterns of the candidate E4-like esterase among resistant and susceptible strains; and (4) to validate the potential insecticide detoxification function provided by the candidate E4-like esterase using transgenic *Drosophila*.

RESULTS

Focal strains

Our study generated eight clonal isofemale strains of *A. kondoi* that were originally collected from a variety of plant hosts and geographically broad locations in Australia (Table 1 and Figure 1a). Resistance in the established isofemale strains was confirmed by screening them against a discriminating dose of the organophosphate insecticide, chlorpyrifos (Supplementary Table S1). Our initial analyses focused on four strains that were collected during the early reports of resistance: Keith, Temora, Kellerberrin and Eudunda. We later added four more strains that were collected

following broader surveys of resistance: Bangham, Coombe, Jung and Moulamein. Based on preliminary bioassays, Keith, Temora, Bangham and Coombe were found to be resistant to organophosphates, carbamates and pyrethroids, while Kellerberrin, Eudunda, Jung and Moulamein were susceptible to these insecticides.

Genome assembly and annotation

To investigate the evolution of insecticide resistance in *A. kondoi*, we generated the first reference genome for this species using the Kellerberrin strain (NCBI Genome Accession, JAUMJG000000000). Our preliminary assessment of genome size for *A. kondoi* was ~452 Mb, with a genomic heterozygosity rate of ~0.87%, based on GENOMESCOPE. Following polishing and purging, our final genome assembly was 443.8 Mb, comprising 615 contigs and 37 scaffolds, with an L50 of 70 sequences and N50 of 1.8 Mb. The mean assembled sequence length was 0.7 Mb, with a minimum of 0.006 Mb and a maximum of 9.7 Mb. Repetitive content comprised 30% of the assembly. In total, we annotated 28,405 genes. The completeness of this gene space was high based on BUSCO scores: 97.5% of arthropod single-copy orthologous genes were present, with 91.7% present as single copies and 5.8% present as duplicate copies. Of these single-copy orthologous genes, 0.9% were fragmented and 1.6% were missing.

Our *A. kondoi* assembly has similar characteristics to genomes developed for the congeneric pea aphid, *A. pisum*, on GenBank. The *A. pisum* GCF_000142985.2 scaffold-level assembly is 541.7 Mb, comprising 60,595 contigs and 23,924 scaffolds, with 20,940 annotated genes. The *A. pisum* GCF_005508785.2 chromosome-level

assembly is 533.6 Mb, comprising 66,716 contigs and 21,227 scaffolds arranged into 4 chromosomes, with 20,307 annotated genes.

Differential gene expression

We compared the transcriptomes of resistant (Keith and Temora) and susceptible (Kellerberrin and Eudunda) strains to identify candidate over-expressed genes linked to resistance. Three major patterns emerged from these transcriptomic analyses. First, the resistant Keith and Temora strains exhibited highly similar gene expression patterns. Second, gene expression patterns between the resistant strains were clearly distinct from those of the two susceptible Kellerberrin and Eudunda strains. Third, the Kellerberrin and Eudunda strains exhibited distinct gene expression patterns relative to each other. These patterns were evident in the clear separation of resistant from susceptible strains on PC axis 1 (41.89% of variation), and the separation of the susceptible strains from each other on PC axis 2 (21.94% of variation) (Figure 1b).

After controlling for false positives, we identified 198 genes that were over-expressed in all four pairwise combinations of resistant versus susceptible strains (Supplementary Table S2). Our GO enrichment analysis did not find any GO term that was over-represented in the top over-expressed genes. However, of interest was an E4-like esterase gene, which was the top over-expressed gene (201-fold greater on average) in all pairwise comparisons between either the Temora or Keith strains and the susceptible Kellerberrin and Eudunda strains. The protein sequence of this *A. kondoi* E4-like esterase showed ~80% similarity to the *M. persicae* E4/FE4 esterase, which is known to contribute to organophosphate, carbamate and pyrethroid

resistance in that species through over-expression (Field and Devonshire 1998; Field and Foster 2002). Similar esterases have also been shown to be over-expressed in other resistant aphid species (Ono et al. 1999; Müller et al. 2023).

Clonal genetic background

We inferred the evolutionary histories among clonal strains by calculating genetic distances using genome-wide biallelic SNPs. For our initial strains (Keith, Temora, Kellerberrin and Eudunda), SNPs were derived from transcriptomes. For the additional strains (Bangham, Coombe, Moulamein, and Jung), SNPs were derived from whole-genome sequencing data. Our comparison of genetic distances among all eight strains indicated that the resistant strains formed a monophyletic lineage that was distinct from all susceptible strains (Figure 1c). Within the resistant and susceptible lineages, genetic differences were comparable across strains for 4,161 biallelic SNP loci. Comparing across resistant strains, the mean allelic differences ranged from 9 to 84.75 alleles, with a mean of 60.31 alleles. Comparing across susceptible strains, the mean allelic differences ranged from 9 to 141.25 alleles, with a mean of 84.82 alleles. When comparing within strains, the mean allelic differences for the four strains with transcriptomic data (Eudunda, Kellerberrin, Temora and Keith) ranged from 11.62 to 17.88 alleles, with a mean of 13.97 alleles. We could not provide the same within-strain assessment for the four strains with whole-genome data (Bangham, Coombe, Jung, Moulamein) because we only sequenced one pooled sample per strain. Across the resistant and susceptible lineages, allelic differences between strains ranged from 3,657 to 3,740 alleles, with a mean of 3,699 alleles.

E4-like esterase genomic copy number, expression, and sequence variation

The identified E4-like esterase was an intriguing candidate for further investigation. given its homology to similar esterases that confer insecticide resistance in other aphids. We used qPCR to validate the over-expression of the E4-like esterase in resistant *A. kondoi* and test whether this over-expression was achieved through increased copy number of this gene. A custom set of primers was designed for the candidate E4-like esterase as our focal gene to be compared against actin as the reference gene – the efficiency of these primers was tested before conducting our experiments (Supplementary Figure S1). We conducted two experiments comparing RNA vs DNA samples: in Experiment 1, samples were comprised of RNA and DNA extracted from single aphids, whereas in Experiment 2, samples were comprised of a pool of two aphids. As expected, RNA (cDNA) samples exhibited $-\Delta C_P$ values that were generally positive for resistant strains and negative for susceptible strains (Figure 2), supporting the hypothesis of over-expression in resistant strain. The relative fold-change estimated between resistant and susceptible strains using the $2^{-\Delta\Delta C_P}$ method (Livak and Schmittgen 2001) (Supplementary Figure S5 and Supplementary Table S3) showed that in Experiment 1, the median fold-change ranged from 127- to 184-fold (mean of 155-fold), and in Experiment 2, the median fold-change ranged from 29- to 124-fold (mean of 75-fold). In contrast, the $-\Delta C_P$ values for DNA samples were ~0 across strains (Figure 2), suggesting that both genes are present at equivalent genomic copy numbers and are amplified at the same rate in qPCR, irrespective of resistance status. This therefore does not support the hypothesis that over-expression

of the E4-like esterase is achieved through increased copy number, so some other regulatory mechanism must therefore be at play.

Closer examination of sequence variation within the E4-like esterase revealed distinct genotypic differences between resistance and susceptible *A. kondoi* strains. A total of five non-synonymous mutations were observed in the candidate E4-like esterase: Ala28Val, Ala61Thr, Met150Leu, Ala527Thr, and Pro586Leu. All resistant strains were homozygous for the alternate allele at codongs 28, 61, 150, 527 and 586, and homozygous for the reference allele at 452 (Figure 3). All susceptible strains had identical genotypes, which comprised homozygous reference alleles for codons 28, 61 and 527, and heterozygous genotypes at codons 150 and 586 (Figure 3).

E4-like esterase transgenesis

Experiments using transgenic *Drosophila melanogaster* were used to functionally validate the role of the *A. kondoi* E4-like esterase in resistance. We successfully established a transgenic strain of *Drosophila* expressing a version of the E4-like esterase containing the Met150Leu and Pro586Leu mutations. Using insecticide bioassays, we demonstrated that expression of this E4-like esterase in the mutant strain conferred significant resistance to all three insecticides, relative to a control strain of the same genetic background but lacking this gene (Table 2 and Figure 4). Specifically, the transgenic *D. melanogaster* expressing the E4-like esterase displayed resistance ratios of 4.31-fold for alpha-cypermethrin, 4.99-fold for chlorpyrifos, and 3.19-fold for pirimicarb.

Target-site mutations

Insecticides typically target specific genes. Organophosphates and carbamates target the acetylcholinesterase (*ace*), and pyrethroids target the para-like voltage-gated sodium channel (*para*). We therefore examined SNPs in the exonic regions of these genes to assess whether any might provide target-site resistance to their associated insecticides. Our genome contained three genes with *ace*/*ace*-like annotations (g46, g11959, and g15835), but none exhibited non-synonymous mutations. Our genome contained two *para* gene annotations (g11612 and g11614), but we only observed three non-synonymous mutations *para* gene g11614: Thr104(1201)Ala, His359(1450)Asn, and His359(1450)Gln. Note that numbers in parentheses are the canonical *para* reference sequence from *Musca domestica*, which is a longer than the *A. kondoi* g11614 *para* protein (Figure S3). Comparison of our two *A. kondoi para* genes with the pest aphids *A. pisum* and *M. persicae* indicated that gene g11614 is the *para* subunit 2, whereas gene g11612 is the *para* subunit 1 (Figure S3). The structure of these two genes in the genome of *A. kondoi* is very similar to that in *A. pisum* and to that described in *M. persicae* (Amey et al. 2015): both genes occur in a proximate genomic region but are on different strands (Figure S4). While susceptible strains were homozygous for the reference mutations in g11614 *para* subunit 2, all resistant strains were heterozygous (Figure S5). These mutations have not been observed in other pyrethroid-resistant arthropods (Dong et al. 2014). Moreover, documented pyrethroid target-site mutations in aphids appear to evolve in subunit 1 (Amey et al. 2015; Zuo et al. 2016; Valmorbida et al. 2022), not subunit 2. We thus take the conservative interpret mutations observed in our study are unlikely

to be involved in pyrethroid resistance, and that there is no evidence for target-site resistance in *A. kondoi* most generally.

DISCUSSION

The evolutionary origins and repeatability of adaptation have long intrigued evolutionary biologists (Cohan and Hoffmann 1989; Korona et al. 1994; Colosimo et al. 2005; Roda et al. 2013; Tepolt et al. 2021). Here, we developed the first reference genome for *A. kondoi,* an economically important global pest, and used this genomic resource to study the evolutionary origins and molecular mechanisms of insecticide resistance in its invasive Australian range. Insecticides are the major way in which *A. kondoi* is managed in Australia agriculture, with organophosphates and carbamates widely used in alfalfa growing regions. This prolonged selection pressure has led to the evolution of resistance, first detected after farmers reported chemical control failures in a small number of field populations in 2018 (Chirgwin et al. 2023). Although not registered to control *A. kondoi* in most cropping situations and thought to be infrequently used against this species in Australia, resistance was also detected to multiple synthetic pyrethroids, namely alpha-cypermethrin and gamma-cyhalothrin (Chirgwin et al. 2023). Insecticide resistance is a trait that is often broadly beneficial in pest organisms due to the use of agrichemicals across large areas (Chevillon et al. 1999; Endersby-Harshman et al. 2020; Zhang et al. 2023). Moreover, clonality in asexual aphids can provide the added benefit of rapidly spreading resistant lineages in local populations and facilitating recovery following major

selection events (Muller 1932; Crow and Kimura 1965; Vorburger 2006; Loxdale 2008; Loxdale et al. 2010).

Our genomic investigation shows that all resistant clonal strains shared a single evolutionary origin and are highly differentiated from all other susceptible clonal strains examined here. This resistant lineage exhibits resistances to all three insecticide classes (organophosphates, carbamates, and pyrethroids), which has undoubtedly given it an advantage in Australia's alfalfa and legume industries that have limited chemical control options. More recently, resistant strains of *A. kondoi* have been collected from very distant sites (~700 km apart) and from different cropping systems (E. Chirgwin, unpub. data), highlighting future issues for resistance to become a problem at a large spatial scale. This spread of a single resistant *A. kondoi* strain is characteristic of superclones in other aphid species. In Australian populations of *Myzus persicae*, more than 300 unique clones have been characterised using microsatellites, yet there is very limited genetic variation among aphids collected from agricultural fields due to sweeps of resistant superclones (Umina et al. 2014; de Little and Umina 2017; Thia, Zhan, et al. 2023). Indeed, over 91% of all *M. persicae* sampled from oilseed rape crops between 2000 and 2024 belong to a single clonal type that has evolved multiple insecticide resistance mechanisms, despite samples being collected from locations more than 3,000 km apart (P. Umina, unpub. data). Similarly, a resistant clone of the English grain aphid, *Sitobion avenae*, has displaced sexually reproducing lineages in the UK, resulting in reduced genetic variation in the field (Morales-Hojas et al. 2020). An important question arising from this work is how long resistance will persist and (or) continue to spread in the field. This will depend on

whether selection pressures can be relaxed to reduce resistance by exploiting costs of resistance, as observed in other arthropod pests (Foster et al. 1999; Bass et al. 2014; Zhang et al. 2015; Maino et al. 2018). However, if the costs of resistance are minimal, resistant *A. kondoi* clones may continue to persist even if insecticide usage is reduced.

The most common mechanisms of evolved insecticide resistance involve target-site changes and the evolution of detoxification mechanisms. In this work, we did not find any clear evidence that resistance in *A. kondoi* is linked to target-site mechanisms. We identified no non-synonymous mutations in any annotated *ace*/*ace*-like genes. The only three non-synonymous mutations detected were in the g11614 *para* gene, but these are not associated with resistance in other arthropods. Instead, our data provide strong evidence that insecticide resistance in *A. kondoi* has evolved through detoxification mechanisms. Through transcriptomic analyses, we identified an E4-like esterase as a candidate gene for resistance. Relative to the susceptible strains, resistant strains exhibited over-expression of this E4-like esterase in the range of 29-fold to 184-fold in qPCR assays and >200-fold in transcriptomic analyses. Our findings not only showed that resistant *A. kondoi* strains over-express this esterase, but they also have a different genotype compared with the susceptible strains. We found no evidence that the E4-like esterase in *A. kondoi* is over-expressed through increased copy number, so another regulatory mechanism must exist.

A particularly interesting feature of the *A. kondoi* esterase is its similarity to the E4/FE4 esterases in *M. persicae,* which are known to be major detoxifiers and sequesters of

organophosphate, carbamate, pyrethroid insecticides (Field and Devonshire 1998; Field and Foster 2002). Homologs of this esterase family have been identified in other aphid species with evolved resistance. In the wheat aphid, *Schizaphis graminum*, an E4/FE4 esterase homolog has been linked to organophophate resistance (Ono et al. 1999). In the pea aphid, *Acyrthosiphum pisum*, two recently described pyrethroid resistant strains appear to over-express an FE4 esterase homolog, although it is still unclear whether this esterase contributes to resistance (Müller et al. 2023). In both *M. persicae* and *S. graminum*, over-expression of these esterases is achieved through gene amplification, with additional regulation through methylation patterns (Hick et al. 1996; Field et al. 1999; Ono et al. 1999; Field 2000). Whilst there appears to be an intriguing macroevolutionary parallelism at the gene family level between *M. persicae*, *S. graminum* and *A. kondoi*, the regulatory mechanism in *A. kondoi* appears to be divergent, given the lack of evidence for gene amplification in its E4-like esterase in this study. Exploring regulatory processes in the *A. kondoi* E4-like esterase is therefore scope for future investigations.

Functional validation of the *A. kondoi* E4-like esterase demonstrated that this enzyme is a general detoxifier of insecticides. In our bioassays, transgenic *Drosophila* ectopically expressing the *A. kondoi* E4-like esterase were significantly more resistant to alpha-cypermethrin (a pyrethroid), chlorpyrifos (an organophosphate), and pirimicarb (a carbamate). This highlights the ability for this esterase to provide cross-resistance across different chemical groups, effectively acting as a pleiotropic gene. In *M. persicae*, the E4 esterase is broadly able to detoxify pyrethroids, organophosphates, and carbamates (Devonshire and Moores 1982). In *S. graminum*,

the E4//FE4-like esterase has only been documented in organophosphate resistance (Siegfried and Ono 1993; Ono et al. 1994). Detoxification enzymes that can provide resistance to many insecticide classes can be highly adaptive in agricultural environments. This is because a key resistance management strategy is to rotate the use of different insecticide classes to reduce selection pressures (Georghiou 1994). However, cross-resistance poses a serious challenge to this strategy because multiple insecticide classes will reinforce selection on the same genetic mechanism. Indeed, since the first detection of resistance, emergency permits for new insecticide classes (e.g., flonicamid and sulfoxaflor) have been issued in efforts to expand chemical control for *A. kondoi* control in Australia.

Our reference genome for *A. kondoi,* together with the detailed transcriptomic analysis, provides an important contribution to the limited genomic resources available for this economically significant aphid species. The high BUSCO score (97.5%) reflects the high quality of our reference genome, with 615 contigs and a total length of 443.8 Mb. This has enabled us to uncover key insights into the genetic mechanisms underlying insecticide resistance and provides a strong foundation for further investigations in this species. Additionally, our characterisation of the E4-like esterase will provide a useful diagnostic molecular marker for screening and monitoring resistance in the field. This marker will facilitate the collection of spatiotemporal data on resistance, providing insights into the dynamics of the persistence of the resistant clone.

CONCLUDING REMARKS

In this work, we disentangled the hypotheses of parallel evolution versus the spread of insecticide resistance in *A. kondoi*, an important agricultural pest. Through genomic and transcriptomic analyses, we revealed that insecticide resistance in *A. kondoi* is driven by detoxification mechanisms: the over-expression of an E4-like esterase with homology to other resistance-conferring esterases in different aphid species. Our work also highlights the rapid spread of a single resistant superclone, reflecting the influence of human-induced selection pressures on pest populations. While our findings suggest a parallel macroevolutionary response to insecticide exposure in *A. kondoi* and other aphid species, they also highlight the unique regulatory mechanisms of the *A. kondoi* E4-like esterase as warranting further investigation. Given the rapid spread of resistance in Australia, there is a need to develop alternative management strategies for *A. kondoi*, including expanding chemical control options and enhancing the use of biological control.

MATERIALS AND METHODS

Focal strains

All strains in this study were maintained as clonal isofemale strains. To purify the resistant strains, artificial selection was imposed on field-collected aphids using leaf dip insecticide bioassays (Umina et al. 2014). Nymphs from Keith, Temora, Bangham and Coombe were exposed to alfalfa leaves dipped in 15 mg a.i./L chlorpyrifos (Lorsban® 500EC, Corteva) for 72 hours. This concentration was previously shown to effectively separate resistant aphids from insecticide-susceptible individuals (Chirgwin

et al. 2023). The chlorpyrifos solution was prepared by diluting 15 mg a.i./L in distilled water. Leaves were dipped in the insecticide solution for 10 seconds and then plated onto 50 mm Petri dishes containing 1% agar. Three dishes were prepared for each strain, each containing three large alfalfa leaves and 10 three-day-old nymphs. After 72 hours, surviving aphids were separated and individually plated on 30 mm Petri dishes with a single untreated alfalfa leaf in agar. Approximately eight days later, individuals that survived and produced nymphs were retained in separate Petri dishes. After three generations, the healthiest surviving replicate was selected as the representative isofemale strain. Isofemale strains were also generated for Kellerberrin, Eudunda, Jung, and Moulamein strains alongside the resistant strains, but these were not exposed to artificial selection. A follow up bioassay using the same discriminating dose of chlorpyrifos (15 mg a.i./L) confirmed Keith and Temora were resistant, while Kellerberrin and Eudunda were susceptible (see Supplementary Table S1).

Genome assembly and annotation

We developed the first reference genome for *A. kondoi* to investigate the genomic basis of insecticide resistance, using the Kellerberrin strain for the assembly. We performed two high molecular weight DNA extractions from 22 and 24 pooled adult aphids, respectively, using the Nanobind® Tissue Kit following a modified 'UHMW DNA Extraction – Dounce Homogenizer' protocol. However, we replaced the Dounce Homogeniser with a simpler homogenisation step, crushing aphids in a 1.5 mL Eppendorf tube with a pestle chilled on ice. The tissue homogenate, lysis buffer, and proteinase K were incubated overnight at 50°C. All other steps were as per the protocol. The DNA was sent to Novogene (Singapore) for library preparation, long-

read sequencing using the Oxford Nanopore Technology (ONT) PromethION platform, and short-read Illumina paired end (150 bp) sequencing on the NovaSeq platform.

We also sequenced a transcriptome from 10 pooled 14-day-old apterous aphids from the Kellerberrin strain. To synchronize aphids, 15 adults were placed onto a 100 mm Petri dish with alfalfa leaves in agar. These aphids were given an initial 24 hours to settle, after which any offspring produced were removed. After a further 24 hours, the adults were removed and any offspring produced were left behind on plates. Offspring were replated every 3 to 4 days, and any showing signs of developing into alates were removed. After 14 days, apterous aphids were pooled, frozen in liquid nitrogen, and sent to AGRF (Australian Genome Research Facility, Melbourne) for RNA extraction, library preparation, and short-read Illumina sequencing (150 bp) on the NovaSeq platform. In total, we obtained 7,076,013 ONT long-reads, 191,891,532 paired reads from the Illumina whole-genome sequencing, and 11,532,979 paired reads from Illumina transcriptome sequencing. Illumina reads were quality trimmed using FASTP v0.23.2 (Chen et al. 2018).

Whole-genome short reads were used to estimate the genome size using a combination of the KMC v3.1.2 (Kokot et al. 2017) and GENOMESCOPE v2 (Vurture et al. 2017) programs. High-quality ONT long-reads were assembled with FLYE v2.9 (Kolmogorov et al. 2019), followed by three iterative polishing steps with whole-genome short reads using PILON v1.23 (Walker et al. 2014). ONT long reads were mapped back onto this assembly with MINIMAP2 v2.17 (Li 2016) and duplicated regions

purged using PURGE_HAPLOTIGS v1.0.4 (Roach et al. 2018). Repetitive regions were annotated using RED v2018.09.10 (Girgis 2015). This constituted our 'curated assembly'. RNA short reads were mapped to the curated assembly with HISAT2 v2.1.0 (Kim et al. 2019). All short-read alignments were filtered for quality (Q20) and duplicate reads and sorted using SAMTOOLS v1.17 (Li et al. 2009; Danecek et al. 2021).

The aligned RNA reads were used to help guide gene annotation with the BRAKER v.2.1.6 pipeline. The output AUGUSTUS (Stanke et al. 2006) gene annotations were retained for downstream analysis. Parsing of annotations and extraction of the longest protein coding transcript was performed through a combination of GFFREAD v0.12.7 (Pertea and Pertea 2020), AGAT v1.1.0 (Dainat 2022), and SEQKIT v2.0.0 (Shen et al. 2016). We assigned function to gene annotations using a combination of BLASTP v0.23.2 (Altschul et al. 1990) and BLAST2GO (Conesa et al. 2005; Conesa and Götz 2008). We downloaded the entire 'nr' database on the 10th of June 2023. We used BLASTP to match the amino acid sequences of the longest transcripts against all arthropod sequences in the 'nr' database. Gene ontology (GO) terms were assigned using INTERPROSCAN v5.59-91.0 (Zdobnov and Apweiler 2001) and revaluated using BLAST2GO. Assembly statistics were generated using QUAST v5.1.0 (Gurevich et al. 2013) and the completeness of single copy ortholog genes was assessed using BUSCO v3.1.0 (Simão et al. 2015).

Differential gene expression

We examined patterns of differential expression among the Keith, Temora, Kellerberrin and Eudunda strains to identify genes contributing to insecticide resistance in *A.*

kondoi. Transcriptomes were derived from pools of 12-day-old apterous aphids. As above, we plated 15 adults onto 100 mm Petri dishes containing alfalfa leaves in agar alfalfa, with a 24-hour settling and culling period, and offspring after 48 hours were removed. These offspring were replated onto 30 mm Petri dishes containing a single alfalfa leaf on agar at densities of five to eight aphids per dish. After 8 days, aphids were moved to larger 50 mm Petri dishes containing two alfalfa leaves on agar. On day 12, apterous aphids from each strain were removed and snap frozen in liquid nitrogen. Four pools of aphids, with each pool comprising approximately 20 to 25 aphids (approximately 10 to 15 mg of tissue). RNA extraction was performed by OzOmics (Melbourne, Australia) using a Monarch® Total RNA Miniprep Kit (New England BioLabs). Library preparation was performed by AGRF (Melbourne) with 150 bp paired-end sequencing on their NovaSeq platform. We successfully derived transcriptomes from all pools except one pool from the Eudunda strain. Hence, $n = 3$ for Eudunda, and $n = 4$ for all other strains. For the successfully sequenced transcriptomes, we obtained 35,232,161 to 52,797,301 raw reads, with a mean of 40,452,782 reads.

Raw transcriptomic reads were trimmed using FASTP. Trimmed transcript reads were then mapped to our assembled reference genome using HISAT2. Mapped reads were filtered to retain high-quality mapped reads (MAPQ ≥ 30) and were sorted using SAMTOOLS. Expression was quantified using STRINGTIE v2.2.1, and the STRINGTIE'S PREPDE.PY script was used to summarise data into a matrix of transcript abundances for all samples. This transcript abundance matrix was imported into *R* for differential

expression analysis among strains. Global patterns of gene expression were visualised by analysing all strains together and performing a PCA on the transcript abundances.

Pairwise comparisons were conducted to identify genes that were differentially expressed between all possible pairs of resistant and susceptible strains (4 total combinations). For each pair, differential expression was analysed using functions from the packages DESEQ2 v1.40.2 (Love et al. 2014) and APEGLM v1.22.1 (Zhu et al. 2019) in *R*. To identify candidate resistant genes, we extracted the top 20 most differentially expressed genes per resistant–susceptible pair based on adjusted *p*-values.

Tests for GO term enrichment were performed on significantly over-expressed genes. Any gene that was significantly over-expressed in 3 out of 4 pairwise comparisons was considered a true outlier, and their GO terms used in enrichment analyses. These analyses were conducted using Fisher's exact test in R with the FISHER.TEST function, and *p*-values adjusted for multiple testing using a Bonferroni correction.

Clonal genetic background

We tested whether resistant strains of *A. kondoi* were derived from the same clonal genetic background. For these analyses, we combined transcriptomic sequencing data from the Keith, Temora, Kellerberrin and Eudunda strains with whole-genome sequencing data from the additional Bangham, Coombe, Jung and Moulamein strains. Whole-genome data for these latter strains was obtained by extracting genomic DNA from 6 pooled adult aphids using a Monarch® Genomic DNA Purification Kit (New England BioLabs), one pool per strain. Whole-genome library

preparation was performed by Novogene (Hong Kong) with 150 bp paired-end sequencing on their NovaSeq platform. We obtained 36,680,245 to 41,806,538 raw reads, with a mean of 40,405,084 reads.

Similar to the transcript reads, whole-genome reads were trimmed with FASTP, mapped with HISAT2, and filtered, sorted and deduplicated with SAMTOOLS. We then called variants in exonic regions by combining the mapped transcript and whole genome reads using BCFTOOLS (Li 2011; Danecek et al. 2021). We then reduced our dataset to only contain SNP (single nucleotide polymorphism) loci with quality scores ≥30 using BCFTOOLS. Variants were imported into R using GENOMALICIOUS v 0.7.8 (Thia and Riginos 2019) and further filtered to only include SNPs with depth ≥15 reads, 0% missing data, and biallelic sites. The final dataset contained 4,161 biallelic SNPs.

Pairwise genetic distances between samples were quantified as the number of allelic differences across all biallelic loci. The pairwise genetic distance matrix was used to derive a UPGMA clustering tree with the PHANGORN v2.12.1 package (Schliep 2011), with negative branch lengths adjusted using the BAT v2.9.6 package (Cardoso et al. 2015). Bootstrapping was undertaken with the APE v 5.8 package (Paradis et al. 2004). The resulting tree was visualised using GGTREE v3.12.0 (Yu et al. 2017) and TREEIO v1.28.0 (Wang et al. 2020).

Target-site mutations

We used our combined transcriptome and whole-genome data to characterise allelic variation in target genes for organophosphate and carbamate insecticides (the acetylcholinesterase gene, *ace*) and pyrethroid insecticides (the *para*-like

voltage-gated sodium channel, *para*). Our assembly of the *A. kondoi* genome identified three genes with *ace* annotations, with gene IDs, g11959, g46, and g15835, and lengths of 822, 706 and 664 amino acids, respectively. There were two genes with *para* annotations, with gene IDs, g11612 and g11614, and lengths of 1,160 and 958 amino acids, respectively. Sequence analysis was performed in R. To determine the relative codon positions of the target gene proteins, we aligned the *A. kondoi* sequences to their respective canonical reference species: *ace* sequences to *Torpedo californica* (X03439) and *para* sequences to *Musca domestica* (NP_001273814). Protein alignments were performed using the MSA v1.36.1 package (Bodenhofer et al. 2015).

We next determined whether missense amino acid changes in our target genes might be associated with insecticide resistance. Here, we considered all possible SNPs (not just biallelic loci) that occurred in the exonic regions of the annotated *ace* and *para* genes. Protein coding annotations were made with SNPEFF (Cingolani et al. 2012). These were then imported into R, where we extracted information about relative codon positions from our *A. kondoi* alignments to canonical reference proteins and matched these to our protein coding annotations using GENOMALICIOUS. We were most interested in any missense mutations that were found in the primary *A. kondoi ace* and *para* gene, especially if they had been previously reported as conferring resistance in the literature.

We only found mutations in one of the *para* genes (see Results). To better contextualise these mutations, we further analytical validated the functional roles of

these annotated *para* genes. Aphids have evolved a heterodimeric *para* sodium channel, controlled by two genes, subunits 1 domains I and II) and 2 (domains III and IV) (Amey et al. 2015). We therefore compared our *A. kondoi para* genes to two other aphids, the congeneric *A. pisum* and *M. persicae*. We used the *Myzus persicae* protein sequences of *para* subunits 1 and 2 (NCBI Protein Accessions CBI71141.1 and CBI71142.1, respectively) (Amey et al. 2015) to query the *Acythrosiphon pisum* genome (NCBI Genome Accession GCF_005508785.1) using NCBI's BLASTP platform. We then recovered two respective top hits, with NCBI Protein Accession XP_029346126.1 (Gene ID 100158802) and XP_001949648.2 (Gene ID 100164620). We then aligned these *M. persicae* and *A. pisum* protein sequences with our *A. kondoi* sequences and that of the canonical *M. domestica* reference sequence, using MSA, visualizing the alignment with GENOMALICIOUS.

E4-like esterase genomic copy number, expression, and sequence variation

Copy number and expression. Our top candidate gene for resistance was an E4-like esterase, which was over-expressed in resistant strains relative to susceptible strains (see Results). We used qPCR to validate the expression levels of the E4-like esterase, and to test whether elevated genomic copy number was driving over-expression. We performed two separate experiments with aphids for qPCR being obtained using the same protocols as those for obtaining transcriptomes (see Section, 'Differential gene expression'). In Experiment 1, we measured individual levels (one aphid per sample) of genomic copy number and expression for the original four strains (Eudunda, Kellerberrin, Keith and Temora) to assess variation within strains. These individual measures also allowed us to test for expression differences between morphs (winged

alate versus non-winged apterous aphids). For each strain, we analysed 24 samples of individual aphids. In Experiment 2, we measured genomic copy number and expression in pooled samples (two aphids per sample) for the additional strains (Jung, Moulamein, Bangham and Coombe), with three of the original strains (Eudunda, Kellerberrin, Keith) included as comparisons. Aphids for both experiments were obtained using the same protocols as those for obtaining transcriptomes (see Section, 'Differential gene expression'). The Temora strain was not included in Experiment 2 due to a lack of nymphs for ageing. In Experiment 2, we analysed 5–6 samples (2 aphids per sample) because our findings from Experiment 1 indicated that individual levels of expression were consistent within strains and that there were no differences among morphs (see Results).

We developed a workflow that allowed us to simultaneously extract both the DNA and RNA from the same sample. Aphid samples (single aphids, or a pool of two aphids) were frozen in liquid nitrogen in a 1.5 mL Eppendorf tube and stored for up to two weeks at –80°C. These were homogenized on ice with a small plastic pestle. The used pestle was then placed into a second Eppendorf tube containing 150µL of 5% Chelex® buffer and proteinase K (20mg/mL, Meridian, CSA-01254; Cincinnati, OH, USA) and swirled in this buffer mix to suspend the residual aphid homogenate − this was used for DNA extraction. We followed the protocol in Yang et al. (2023) for Chelex® DNA extraction.

Simultaneously, 200 µL of RNA protection reagent from the Monarch® Total RNA Miniprep Kit (New England BioSciences, Notting Hill, VIC, Australia; #T2010) was

added directly to the homogenized aphid tissue in the original sample tube; this was used for RNA extraction. We performed RNA extraction following the Monarch® Total RNA Miniprep Kit protocol. Extracted RNA was converted into cDNA using the ThermoFisher Scientific High-Capacity cDNA Reverse Transcription Kit (Parkville, VIC, Australia; #4368814) as per manufacturer's instructions.

We used qPCR to quantify the relative expression of the candidate E4-like esterase across clonal strains of *A. kondoi*. DNA extractions were diluted 1:3, and cDNA samples were diluted 1:10, with PCR water. A set of primers for the target gene were designed in GENEIOUS PRIME for the E4 esterase: Akond_E4_F, CCTCGTCTTGGGTAACACTCA, and Akond_E4_R, CATTTTCGCCGTTTGGTCCA. The aphid actin gene provided a reference gene with primers from (Yang et al. 2023): actin_aphid_F1, GTGATGGTGTATCTCACACTGTC; and actin_aphid_R1, AGCAGTGGTGGTGAAACTG. Our qPCR reactions were performed according to Lee et al. (2012) with a Roche LightCycler 480. Briefly, 10-minute incubation at 95°C was used to heat activate the quick start IMMOLASE (Meridian, BIO-21047; Cincinnati, OH, USA), which was followed by 45 cycles of 95°C for 10 seconds, 54°C for 20 seconds, and 72°C for 15 seconds. The cycle ended with a high-resolution melt of 95°C for 1 minute (ramp rate = 4.8°C/second), 40°C for 1 minute (ramp rate = 2.5°C), and then an increase to 65°C (ramp rate = 4.8°C/second). Fluorescence data was collected continuously from 65°C to 95°C (ramp rate = 0.02°C/second, 25 acquisitions per °C). Prior to our main experiment, we validated the amplification efficiency of primers using the Kellerberrin strain (Supplementary Figure S1).

A mean C_P (crossing-point) value for each aphid was calculated over two replicate qPCR reactions. We calculated the $-\Delta C_P$ as –(E4 esterase C_P – actin C_P) for each aphid. The $2^{-\Delta\Delta C_P}$ method (Livak and Schmittgen 2001) was used to estimate the relative expression (fold-change) between resistant and susceptible strains. We calculated the $2^{-\Delta\Delta C_P}$ between each pair of resistant vs susceptible strains within each experiment. Within a strain comparison, we calculated $2^{-\Delta\Delta C_P}$ between all pairs of aphids from both strains. This allowed us to obtain a median value with 2.5% and 97.5% percentiles for the estimated $2^{-\Delta\Delta C_P}$.

Sequence variation. We characterised the distribution of segregating polymorphism in the exonic regions of our candidate E4-like esterase among all eight strains. We used the genetic variants from our genomic analyses and determined the protein coding effects through custom R code, combining the R packages BIOSTRINGS, DATA.TABLE (Dowle and Srinivasan 2019), TIDYVERSE (Wickham et al. 2019), and SEQINR (Charif and Lobry 2007), and GENOMALICIOUS.

E4-like esterase transgenesis

Ectopic expression of our candidate E4-like esterase in *Drosophila melanogaster* (herein, '*Drosophila*') was used to validate its role in insecticide resistance. Our analysis of sequence variation in the candidate E4-like esterase revealed non-synonymous differences between the susceptible and resistance *A. kondoi* strains (see Results). We were able to successfully obtain a strain of *D. melanogaster* carrying an E4-like esterase sequence that was nearly identical to the reference esterase annotation but contained a Met150Leu and Pro586Leu mutation.

The E4-like esterase was synthesised (Twist Bioscience) and cloned into the pUASTattB plasmid between EcoRI and XbaI sites. (GenBank: EF362409.1). The construct was then transformed into the *Drosophila* germline, which carried an attP docking site on chromosome 2 (attP40) and the phiC31 integrase gene under the control of the vasa regulatory region on the X chromosome (y w M (eGFP, vas-int, dmRFP)ZH-2A: P [CaryP]attP40). Transgenic strains were balanced, and the integration of the transgenes confirmed using PCR and sequencing.

Virgin females of the Act5C-GAL4 strain ("y[1] w[∗]; P(Act5C-GAL4-w)E1/CyO,""1;2") (Bloomington Stock Center) were crossed with UAS-E4-like males to allow mating and oviposition. Bioassays, using 6 concentrations of technical grade pirimicarb, chlorpyrifos or alpha-cypermethrin, were performed to assess the susceptibility of transgenic adult female flies to these compounds. The insecticide solutions were diluted in water and overlaid on 1.5% agar (1% sucrose, 0.5% acetic acid) in standard fly vials, then allowed to dry at room temperature overnight. Twenty adult females (2-7 days post-eclosion) were added to each vial, and mortality assessed after 48 hours (alpha-cypermethrin) or 72 hours (pirimicarb and chlorpyrifos). Five replicates were conducted for each concentration. A *Drosophila* strain of the same genetic background as the two transgenic strains, but lacking a transgene (progeny of crosses of the Act5C-GAL4 and UAS-no transgene strains), was included in all bioassays as a reference control. Control mortality was assessed using vials containing agar but lacking insecticide.

Dose-response data was analysed in R. For each insecticide and *Drosophila* strain combination, we fitted a quasibinomial model with mortality as a function of the log10-transformed insecticide concentration, using the GLM function from the STATS package. We derived χ^2 goodness-of-fit test statistics and *p*-values (Brown 1978) using custom code. LD50-values were obtained with the DOSE.P function from the MASS package. Resistance ratios for the mutant strain were calculated as the mutant LD50-value divided by the control LD50-value for each insecticide.

ACKNOWLEDGEMENTS

We thank Alex Gill from the University of Melbourne for his advice and support on culturing *A. kondoi* in the lab. This work was supported by funding through the University of Melbourne's 'Early Carer Researcher Global Collaborations Award' (JAT), investment from the Grains Research and Development Corporation through the 'Australian Grain Pest Innovation Program' (AAH and PAU). AgriFutures Australia provided additional financial support for sample collection (EC and PAU). For the purpose of open access, the authors have applied a 'Creative Commons Attribution (CC BY) licence to any Author Accepted Manuscript version arising from this submission.

CONTRIBUTIONS

University of Melbourne. JAT, AAH and PAU conceptualised the project. PAU, AAH and JAT acquired funding and performed project administration. PAU oversaw the preliminary characterisation of resistance in *A. kondoi*. JAT developed the isofemale strains of *Acythosiphon kondoi* used in this study. JAT prepared all samples for transcriptomic and genomic sequencing. JAT co-led the genome assembly and differential expression analysis. JAT led the analysis of clonal genetic backgrounds, experimental design and analysis of E4-like esterase expression and copy number validation, analysis of target-site mutations, analysis of sequence variation in the E4-like esterase, and analysis of dose-responses of transgenic *Drosophila*. CJB led the development of molecular protocols for validating E4-like esterase expression and copy number. Culturing and molecular work associated with validating expression and copy number was contributed to by CJB, LAS, MS, KR, CJ, APSD, and QY. The original version of this manuscript was written by JAT, with contributions from PAU and AAH, and additional comments made by CJB, LAS, MS, KR, CJ, APSD, and QY.

University of Exeter. BJH co-led the genome assembly and differential expression analysis. SW and BT designed and executed the chemical bioassays of transgenic *Drosophila*. CB hosted JAT at the University of Exeter to work on the genomic analyses. Contributions to original manuscript was made by CB, with additional comments made by BJH, BT, and SW.

Cesar Australia. EC performed the original field collections of *A. kondoi* and identified the discriminating doses used to separate resistant from susceptible clones. MB

contributed to molecular associated with validating expression and copy number. Additional comments to the manuscript were made by EC and MB.

DATA AVAILABILITY

The reference genome for *Acrythosiphon kondoi* that was generated in this study has been deposited into GenBank Genomes (JAUMJG000000000). Genomic and transcriptomic reads associated with this work have been submitted to GenBank BioProject PRJNA989388. The accession details for all read data can be found in 'Appendix_NCBI_accessions.xlsx'. Data and scripts associated with this work are archived in a Dryad repository (Thia 2024, DOI: 10.5061/dryad.c59zw3rjr).

REFERENCES

Altschul SF, Gish W, Miller W, Myers EW, Lipman DJ. 1990. Basic local alignment search tool. *J Mol Biol* 215:403–410.

Amey JS, O'Reilly AO, Burton MJ, Puinean AM, Mellor IR, Duce IR, Field LM, Wallace BA, Williamson MS, Davies TGE. 2015. An evolutionarily-unique heterodimeric voltage-gated cation channel found in aphids. *FEBS Lett* 589:598–607.

Barraclough TG, Birky W, Burt A. 2003. Diversification in sexual and asexual organisms. *Evolution (N Y)* 57:2166–2172.

Bass C, Puinean AM, Zimmer CT, Denholm I, Field LM, Foster SP, Gutbrod O, Nauen R, Slater R, Williamson MS. 2014. The evolution of insecticide resistance in the peach potato aphid, *Myzus persicae*. *Insect Biochem Mol Biol* 51:41–51.

Blackman RL, Eastop VF. 2017. Taxonomic issues. In: Van Emden HF, Harrington R, editors. Aphids as Crop Pests. Wallingford, Oxfordshire, UK, and Cambridge, Massachusetts, USA: CABI Publishing. p. 1–29.

Bodenhofer U, Bonatesta E, Horejš-Kainrath C, Hochreiter S. 2015. msa: an R package for multiple sequence alignment. *Bioinformatics* 31:3997–3999.

Bontrager M, Angert AL. 2019. Gene flow improves fitness at a range edge under climate change. *Evol Lett* 3:55–68.

Brown CC. 1978. The Statistical Analysis of Dose-Effect Relationships. In: Principles of Ecotoxicology. London: John Wiley and Sons. p. 115–148.

Caballero JD, Clark ST, Coburn B, Zhang Y, Wang PW, Donaldson SL, Elizabeth Tullis D, Yau YCW, Waters VJ, Hwang DM, et al. 2015. Selective sweeps and parallel pathoadaptation drive pseudomonas aeruginosa evolution in the cystic fibrosis lung. *mBio* 6:e00981-15.

Cardoso P, Rigal F, Carvalho JC. 2015. BAT–Biodiversity Assessment Tools, an R package for the measurement and estimation of alpha and beta taxon, phylogenetic and functional diversity. *Methods Ecol Evol* 6:232–236.

Charif D, Lobry JR. 2007. SeqinR 1.0-2: a contributed package to the R project for statistical computing devoted to biological sequences retrieval and analysis. In:

Structural approaches to sequence evolution: Molecules, networks, populations. Springer. p. 207–232.

Chen S, Zhou Y, Chen Y, Gu J. 2018. fastp: an ultra-fast all-in-one FASTQ preprocessor. *Bioinformatics* 34:i884–i890.

Chevillon C, Raymond M, Guillemaud T, Lenormand T, Pasteur N. 1999. Population genetics of insecticide resistance in the mosquito. *Biological Journal of the Linnean Society* 68:147–157.

Chirgwin E, Thia JA, Copping K, Umina PA. 2023. Discovery of insecticide resistance in field-collected populations of the aphid pest, *Acyrthosiphon kondoi* Shinji. *Pest Manag Sci* 80:1338–1347.

Cingolani P, Platts A, Wang LL, Coon M, Nguyen T, Wang L, Land SJ, Lu X, Ruden DM. 2012. A program for annotating and predicting the effects of single nucleotide polymorphisms, SnpEff: SNPs in the genome of Drosophila melanogaster strain w1118; iso-2; iso-3. *Fly (Austin)* 6:80–92.

Cohan FM, Hoffmann AA. 1989. Uniform selection as a diversifying force in evolution: evidence from Drosophila. *Am Nat* 134:613–637.

Colosimo PF, Hosemann KE, Balabhadra S, Villarreal G, Dickson M, Grimwood J, Schmutz J, Myers RM, Schluter D, Kingsley DM. 2005. Widespread Parallel Evolution in Sticklebacks by Repeated Fixation of Ectodysplasin Alleles. *Science (1979)* 307:1928–1933.

Conesa A, Götz S. 2008. Blast2GO: a comprehensive suite for functional analysis in plant genomics. *Int J Plant Genomics* 2008.

Conesa A, Götz S, García-Gómez JM, Terol J, Talón M, Robles M. 2005. Blast2GO: a universal tool for annotation, visualization and analysis in functional genomics research. *Bioinformatics* 21:3674–3676.

Crossley MS, Chen YH, Groves RL, Schoville SD. 2017. Landscape genomics of Colorado potato beetle provides evidence of polygenic adaptation to insecticides. *Mol Ecol*:6284–6300.

Crow JF, Kimura M. 1965. Evolution in sexual and asexual organisms. *Am Nat*:439–450.

Dainat J. 2022. AGAT: Another Gff Analysis Toolkit to handle annotations in any GTF/GFF format. *Zenodo*.

Danecek P, Bonfield JK, Liddle J, Marshall J, Ohan V, Pollard MO, Whitwham A, Keane T, McCarthy SA, Davies RM. 2021. Twelve years of SAMtools and BCFtools. *Gigascience* 10:giab008.

Davies TGE, Field LM, Usherwood PNR, Williamson MS. 2007. DDT, pyrethrins, pyrethroids and insect sodium channels. *IUBMB Life* 59:151–162.

Devonshire AL, Moores GD. 1982. A carboxylesterase with broad substrate specificity causes organophosphorus, carbamate and pyrethroid resistance in peach-potato aphids (*Myzus persicae*). *Pestic Biochem Physiol* 18:235–246.

Dong K, Du Y, Rinkevich F, Nomura Y, Xu P, Wang L, Silver K, Zhorov BS. 2014. Molecular biology of insect sodium channels and pyrethroid resistance. *Insect Biochem Mol Biol* [Internet] 50:1–17. Available from: http://dx.doi.org/10.1016/j.ibmb.2014.03.012

Dowle M, Srinivasan A. 2019. data.table: Extension of "data.frame."

Endersby-Harshman NM, Schmidt TL, Chung J, van Rooyen A, Weeks AR, Hoffmann AA. 2020. Heterogeneous genetic invasions of three insecticide resistance mutations in Indo-Pacific populations of Aedes aegypti (L.). *Mol Ecol* 29:1628–1641.

Feliziani S, Marvig RL, Luján AM, Moyano AJ, Di Rienzo JA, Krogh Johansen H, Molin S, Smania AM. 2014. Coexistence and Within-Host Evolution of Diversified Lineages of Hypermutable *Pseudomonas aeruginosa* in Long-term Cystic Fibrosis Infections. *PLoS Genet* 10.

Feyereisen R, Dermauw W, Van Leeuwen T. 2015. Genotype to phenotype, the molecular and physiological dimensions of resistance in arthropods. *Pestic Biochem Physiol* 121:61–77.

Field LM. 2000. Methylation and expression of amplified esterase genes in the aphid *Myzus persicae* (Sulzer). *Biochemical Journal* 349:863–868.

Field LM, Blackman RL, Tyler-Smith C, Devonshire AL. 1999. Relationship between amount of esterase and gene copy number in insecticide-resistant *Myzus persicae* (Sulzer). *Biochemical Journal* 339:737–742.

Field LM, Devonshire AL. 1998. Evidence that the E4 and FE4 esterase genes responsible for insecticide resistance in the aphid *Myzus persicae* (Sulzer) are part of a gene family. *Biochemical Journal* 330:169–173.

Field LM, Foster SP. 2002. Amplified esterase genes and their relationship with other insecticide resistance mechanisms in English field populations of the aphid, *Myzus persicae* (Sulzer). *Pest Manag Sci* 58:889–894.

Foster SP, Woodcock CM, Williamson MS, Devonshire AL, Denholm I, Thompson R. 1999. Reduced alarm response by peach-potato aphids, *Myzus persicae* (Hemiptera: Aphididae), with knock-down resistance to insecticides (kdr) may impose a fitness cost through increased vulnerability to natural enemies. *Bull Entomol Res* 89:133–138.

Fournier D. 2005. Mutations of acetylcholinesterase which confer insecticide resistance in insect populations. *Chem Biol Interact* 157–158:257–261.

Georghiou GP. 1994. Principles of insecticide resistance management. *Phytoprotection* 75:51–59.

Gerrish PJ, Lenski RE. 1998. The fate of competing beneficial mutations in an asexual population. *Genetica* 102:127–144.

Gilabert A, Dedryver CA, Stoeckel S, Plantegenest M, Simon JC. 2015. Longitudinal clines in the frequency distribution of “super-clones” in an aphid crop pest. *Bull Entomol Res* 105:694–703.

Girgis HZ. 2015. Red: an intelligent, rapid, accurate tool for detecting repeats de-novo on the genomic scale. *BMC Bioinformatics* [Internet] 16:227. Available from: https://doi.org/10.1186/s12859-015-0654-5

Godefroid M, Meynard CN, Clamens AL, Popkin M, Jousselin E. 2024. On the role of niche specialization in the geographic distribution of aphid asexual lineages: a case study using the leaf-curl plum aphid superclones. *Oikos* 2024.

Gurevich A, Saveliev V, Vyahhi N, Tesler G. 2013. QUAST: Quality assessment tool for genome assemblies. *Bioinformatics* 29:1072–1075.

Hick CA, Field LM, Devonshire AL. 1996. Changes in the methylation of amplified esterase DNA during loss and reselection of insecticide resistance in peach-potato aphids, Myzus persicae. *Insect Biochem Mol Biol* 26:41–47.

Hoffmann AA, Reynolds KT, Nash MA, Weeks AR. 2008. A high incidence of parthenogenesis in agricultural pests. *Proceedings of the Royal Society B: Biological Sciences* 275:2473–2481.

Howe DK, Sibley LD. 1995. Toxoplasma gondii Comprises Three Clonal Lineages: Correlation of Parasite Genotype with Human Disease. *J Infect Dis* 172:1561–1566.

Humphries AW, Peck DM, Robinson SS, Rowe T, Oldach K. 2012. A new biotype of bluegreen aphid (*Acyrthosiphon kondoi* Shinji) found in south-eastern Australia overcomes resistance in a broad range of pasture legumes. *Crop Pasture Sci* 63:893–901.

Huse HK, Kwon T, Zlosnik JEA. 2010. Parallel Evolution in Pseudomonas aeruginosa over 39,000 Generations In Vivo. *mBio* 1:e00199-10.

Kawada K. 1992. Production of sexuals in the aphid Acyrthosiphon kondoi in Japan (Homoptera: Aphidinea: Aphididae). *Entomologia Generalis* 17:115–119.

Khan A, Taylor S, Ajioka JW, Rosenthal BM, Sibley LD. 2009. Selection at a single locus leads to widespread expansion of *Toxoplasma gondii* lineages that are virulent in mice. *PLoS Genet* 5:1–14.

Kim D, Paggi JM, Park C, Bennett C, Salzberg SL. 2019. Graph-based genome alignment and genotyping with HISAT2 and HISAT-genotype. *Nature Biotechnologyotechnology* 37:907–915.

Kokot M, Długosz M, Deorowicz S. 2017. KMC 3: counting and manipulating k-mer statistics. *Bioinformatics* 33:2759–2761.

Kolmogorov M, Yuan J, Lin Y, Pevzner PA. 2019. Assembly of long, error-prone reads using repeat graphs. *Nat Biotechnol* 37:540–546.

Korona R, Nakatsu CH, Forney LJ, Lenski RE. 1994. Evidence for multiple adaptive peaks from populations of bacteria evolving in a structured habitat. *Proceedings of the National Academy of Sciences* 91:9037–9041.

Korpelainen H. 1986. Competition between clones: An experimental study in a natural population of *Daphnia magna*. *Hereditas* 105:29–35.

Lee SF, White VL, Weeks AR, Hoffmann AA, Endersby NM. 2012. High-throughput PCR assays to monitor Wolbachia infection in the dengue mosquito (*Aedes aegypti*) and *Drosophila simulans*. *Appl Environ Microbiol* 78:4740–4743.

Li H. 2011. A statistical framework for SNP calling, mutation discovery, association mapping and population genetical parameter estimation from sequencing data. *Bioinformatics* 27:2987–2993.

Li H. 2016. Minimap and miniasm: fast mapping and de novo assembly for noisy long sequences. *Bioinformatics* 32:2103–2110.

Li H, Handsaker B, Wysoker A, Fennell T, Ruan J, Homer N, Marth G, Abecasis G, Durbin R. 2009. The sequence alignment/map format and SAMtools. *Bioinformatics* 25:2078–2079.

de Little SC, Edwards O, van Rooyen AR, Weeks A, Umina PA. 2017. Discovery of metabolic resistance to neonicotinoids in green peach aphids (*Myzus persicae*) in Australia. *Pest Manag Sci* 73:1611–1617.

de Little SC, Umina PA. 2017. Susceptibility of Australian *Myzus persicae* (Hemiptera: Aphididae) to Three Recently Registered Insecticides: Spirotetramat, Cyantraniliprole, and Sulfoxaflor. *J Econ Entomol* 110:1764–1769.

Livak KJ, Schmittgen TD. 2001. Analysis of relative gene expression data using real-time quantitative PCR and the 2<super>–ΔΔCT</super>method. *Methods* 25:402–408.

Love MI, Huber W, Anders S. 2014. Moderated estimation of fold change and dispersion for RNA-seq data with DESeq2. *Genome Biol* 15:1–21.

Loxdale HD. 2008. The nature and reality of the aphid clone: Genetic variation, adaptation and evolution. *Agric For Entomol* 10:81–90.

Loxdale HD, Massonnet B, Weisser WW. 2010. Why are there so few aphid clones? *Bull Entomol Res* 100:613–622.

Lyberger K, Schoener TW. 2023. Differential genotype response to increased resource abundance helps explain parallel evolution of *Daphnia* populations in the wild. *Ecol Evol* 13:1–9.

Magalhaes IS, Whiting JR, D'Agostino D, Hohenlohe PA, Mahmud M, Bell MA, Skúlason S, MacColl ADC. 2020. Intercontinental genomic parallelism in multiple three-spined stickleback adaptive radiations. *Nat Ecol Evol*.

Mahieu L, González-González A, Rubio-Meléndez ME, Moya-Hernández M, Francis F, Ramírez CC. 2024. An Aphid Pest Superclone Benefits From a Facultative Bacterial Endosymbiont in a Host-Dependent Manner, Leading to Reproductive and Proteomic Changes. *Arch Insect Biochem Physiol* 117:e22154.

Maino JL, Umina PA, Hoffmann AA. 2018. Climate contributes to the evolution of pesticide resistance. *Global Ecology and Biogeography* 27:223–232.

Montejo-Kovacevich G, Meier JI, Bacquet CN, Warren IA, Chan YF, Kucka M, Salazar C, Rueda-M N, Montgomery SH, McMillan WO, et al. 2022. Repeated genetic adaptation to altitude in two tropical butterflies. *Nat Commun* 13:1–16.

Morales-Hojas R, Chen J, Sun J, Alvira F, Xiaoling I. 2020. Contrasting population structure and demographic history of cereal aphids in different environmental and agricultural landscapes. *Ecol Evol* 10:9647–9662.

Muller HJ. 1932. Some genetic aspects of sex. *Am Nat* 66:118–138.

Müller V, Buer B, Lueke B, Mazzoni E, Pym A, Bass C, Nauen R. 2023. Molecular characterization of pyrethroid resistance in field-collected populations of the pea aphid, *Acyrthosiphon pisum*. *Entomol. Gen* 43:627–637.

Natwick E, Brlow V, Godfrey L, Goddell P, Long R. 2014. Blue alfalfa aphid: Old pest with new management challenges. In: California Alfalfa, Forage, and Grain Symposium. Long Beach, California, USA.

Nguyen Ba AN, Cvijović I, Rojas Echenique JI, Lawrence KR, Rego-Costa A, Liu X, Levy SF, Desai MM. 2019. High-resolution lineage tracking reveals travelling wave of adaptation in laboratory yeast. *Nature* 575:494–499.

Ono M, Richman JS, Siegfried BD. 1994. In Vitro Metabolism of Parathion in Susceptible and Parathion-Resistant Strains of the Greenbug, *Schizaphis graminum* (Rondani) (Homoptera: Aphididae). *Pestic Biochem Physiol* [Internet] 49:191–197. Available from: https://www.sciencedirect.com/science/article/pii/S0048357584710479

Ono M, Swanson JJ, Field LM, Devonshire AL, Siegfried BD. 1999. Amplification and methylation of an esterase gene associated with insecticide-resistance in greenbugs, *Schizaphis graminum*(Rondani) (Homoptera: Aphididae). Available from: www.elsevier.com/locate/ibmb

Paradis E, Claude J, Strimmer K. 2004. APE: analyses of phylogenetics and evolution in R language. *Bioinformatics* 20:289–290.

Pertea G, Pertea M. 2020. GFF utilities: GffRead and GffCompare. *F1000Res* 9.

Rispe C, Pierre J -S., Simon J -C., Gouyon P -H. 1998. Models of sexual and asexual coexistence in aphids based on constraints. *J Evol Biol* 11:685–701.

Rispe C, Pierre J-S. 1998. Coexistence between cyclical parthenogens, obligate parthenogens, and intermediates in a fluctuating environment. *J Theor Biol* 195:97–110.

Roach MJ, Schmidt S, Borneman AR. 2018. Purge Haplotigs: Synteny Reduction for Third-gen Diploid Genome Assemblies. *BMC Bioinformatics* 19:1–10.

Roda F, Liu H, Wilkinson MJ, Walter GM, James ME, Bernal DM, Melo MC, Lowe A, Rieseberg LH, Prentis P, et al. 2013. Convergence and divergence during the adaptation to similar environments by an Australian groundsel. *Evolution (N Y)* 67:2515–2529.

Ryalls JMW, Riegler M, Moore BD, Johnson SN. 2013. Biology and trophic interactions of lucerne aphids. *Agric For Entomol* 15:335–350.

Schliep KP. 2011. phangorn: phylogenetic analysis in R. *Bioinformatics* 27:592–593.

Shen W, Le S, Li Y, Hu F. 2016. SeqKit: a cross-platform and ultrafast toolkit for FASTA/Q file manipulation. *PLoS One* 11:e0163962.

Siegfried BD, Ono M. 1993. Mechanisms of Parathion Resistance in the Greenbug, *Schizaphis graminum* (Rondani). *Pestic Biochem Physiol* 45:24–33.

Simão FA, Waterhouse RM, Ioannidis P, Kriventseva E V., Zdobnov EM. 2015. BUSCO: Assessing genome assembly and annotation completeness with single-copy orthologs. *Bioinformatics* 31:3210–3212.

Singh KS, Cordeiro EMG, Troczka BJ, Pym A, Mackisack J, Mathers TC, Duarte A, Legeai F, Robin S, Bielza P, et al. 2021. Global patterns in genomic diversity underpinning the evolution of insecticide resistance in the aphid crop pest *Myzus persicae*. *Commun Biol*:1–16.

Sprengelmeyer QD, Pool JE. 2021. Ethanol resistance in Drosophila melanogaster has increased in parallel cold-adapted populations and shows a variable genetic architecture within and between populations. *Ecol Evol* 11:15364–15376.

Stanke M, Keller O, Gunduz I, Hayes A, Waack S, Morgenstern B. 2006. AUGUSTUS: ab initio prediction of alternative transcripts. *Nucleic Acids Res* 34:W435–W439.

Steiner CF, Stockwell RD, Tadros M, Shaman L, Patel K, Khraizat L. 2016. Impacts of dispersal on rapid adaptation and dynamic stability of *Daphnia* in fluctuating environments. *Proceedings of the Royal Society B: Biological Sciences* 283.

Tepolt CK, Grosholz E, de Rivera C, Ruiz G. 2021. Balanced polymorphism fuels rapid selection in an invasive crab despite high gene flow and low genetic diversity. *Mol Ecol*:1–15.

Thia JA. 2024. Dataset for: Spread of a single superclone drives insecticide resistance in Acyrthosiphon kondoi across an invasive range. *Data Dryad*.

Thia JA, Korhonen PK, Young ND, Gasser RB, Umina PA, Yang Q, Edwards O, Tom W, Hoffmann AA. 2023. The redlegged earth mite draft genome provides new insights into pesticide resistance evolution and demography in its invasive Australian range. *J Evol Biol* 36:381–398.

Thia JA, Riginos C. 2019. *genomalicious*: serving up a smorgasbord of R functions for population genomic analyses. *bioRxiv*:667337.

Thia JA, Zhan D, Robinson K, Umina PA, Hoffmann AA, Yang Q. 2023. "Drifting" *Buchnera* genomes track the microevolutionary trajectories of their aphid hosts. *bioRxiv*.

Umina PA, Edwards O, Carson P, Van Rooyen A, Anderson A. 2014. High levels of resistance to carbamate and pyrethroid chemicals widespread in Australian *Myzus persicae* (Hemiptera: Aphididae) populations. *J Econ Entomol* 107:1626–1638.

Valmorbida I, Hohenstein JD, Coates BS, Bevilaqua JG, Menger J, Hodgson EW, Koch RL, O'Neal ME. 2022. Association of voltage-gated sodium channel mutations with field-evolved pyrethroid resistant phenotypes in soybean aphid and genetic markers for their detection. *Sci Rep* 12.

Vorburger C. 2006. Temporal dynamics of genotypic diversity reveal strong clonal selection in the aphid *Myzus persicae*. *J Evol Biol* 19:97–107.

Vurture GW, Sedlazeck FJ, Nattestad M, Underwood CJ, Fang H, Gurtowski J, Schatz MC. 2017. GenomeScope: fast reference-free genome profiling from short reads. *Bioinformatics* 33:2202–2204.

Walker BJ, Abeel T, Shea T, Priest M, Abouelliel A, Sakthikumar S, Cuomo CA, Zeng Q, Wortman J, Young SK. 2014. Pilon: an integrated tool for comprehensive microbial variant detection and genome assembly improvement. *PLoS One* 9:e112963.

Walsh TK, Joussen N, Tian K, Mcgaughran A, Anderson CJ, Qiu X, Ahn S-J, Bird L, Pavlidi N, Vontas J, et al. 2018. Multiple recombination events between two cytochrome P450 loci contribute to global pyrethroid resistance in *Helicoverpa armigera*. *PLoS One* 13:e0197760.

Wang L-G, Lam TT-Y, Xu S, Dai Z, Zhou L, Feng T, Guo P, Dunn CW, Jones BR, Bradley T. 2020. Treeio: an R package for phylogenetic tree input and output with richly annotated and associated data. *Mol Biol Evol* 37:599–603.

Ward S, Jalali T, van Rooyen A, Reidy-Crofts J, Moore K, Edwards O, Umina PA. 2024. The evolving story of sulfoxaflor resistance in the green peach aphid, Myzus persicae (Sulzer). *Pest Manag Sci* 80:866–873.

Wickham H, Averick M, Bryan J, Chang W, McGowan L, François R, Grolemund G, Hayes A, Henry L, Hester J. 2019. Welcome to the Tidyverse. *J Open Source Softw* 4:1686.

Williams I, Dixon A. 2017. Life Cycles and Polymorphism. In: Van Emden HF, Harrington R, editors. Aphids as Crop Pests. Wallingford, Oxfordshire, UK, and Cambridge, Massachusetts, USA: CABI Publishing. p. 69–81.

Yang Q, Gill A, Robinson KL, Umina PA, Ross PA, Zhan D, Brown C, Bell N, MacMahon A, Hoffmann AA. 2023. A diversity of endosymbionts across Australian aphids and their persistence in aphid cultures. *Environ Microbiol*:1988–2001.

Yang Q, Umina PA, Rašić G, Bell N, Fang J, Lord A, Hoffmann AA. 2020. Origin of resistance to pyrethroids in the redlegged earth mite (*Halotydeus destructor*) in Australia: repeated local evolution and migration. *Pest Manag Sci*.

Yu G, Smith DK, Zhu H, Guan Y, Lam TT. 2017. ggtree: an R package for visualization and annotation of phylogenetic trees with their covariates and other associated data. *Methods Ecol Evol* 8:28–36.

Zdobnov EM, Apweiler R. 2001. InterProScan–an integration platform for the signature-recognition methods in InterPro. *Bioinformatics* 17:847–848.

Zhang L, Li Z, Peng Y, Liang X, Wilson K, Chipabika G, Karangwa P, Uzayisenga B, Mensah BA, Kachigamba DL, et al. 2023. Global genomic signature reveals the evolution of fall armyworm in the Eastern hemisphere. *Mol Ecol* 32:5463–5478.

Zhang LJ, Jing YP, Li XH, Li CW, Bourguet D, Wu G. 2015. Temperature-sensitive fitness cost of insecticide resistance in Chinese populations of the diamondback moth *Plutella xylostella*. *Mol Ecol* 24:1611–1627.

Zhu A, Ibrahim JG, Love MI. 2019. Heavy-tailed prior distributions for sequence count data: removing the noise and preserving large differences. *Bioinformatics* 35:2084–2092.

Zuo Y, Peng X, Wang K, Lin F, Li Y, Chen M. 2016. Expression patterns, mutation detection and RNA interference of Rhopalosiphum padi voltage-gated sodium channel genes. *Sci Rep* 6.

TABLES AND FIGURES

Table 1. Clonal *Acyrthosiphon kondoi* strains examined in this study. Strains are organised by resistance status, sampling location and date, and host plant collected from in the field. Note, blank latitudes or longitudes indicate lack of specific geolocation data.

Resistance status	Strain	State	Latitude	Longitude	Date collected (YYYY-MM-DD)	Host plant
Resistant	Bangham	SA	–36.49	140.88	2021-09-14	*Trifolium subterraneum*
	Coombe	SA	–35.95	140.32	2022-08-17	*Medicago sativa*
	Keith	SA	–36.10	140.37	2020-12-21	*Medicago sativa*
	Temora	NSW	–34.56	147.60	2020-06-29	*Medicago sativa*
Susceptible	Eudunda	SA	–34.14	139.00	2022-09-03	*Vicia sativa*
	Jung	VIC	–36.55	142.36	2022-10-18	*Lens culinaris*
	Kellerberrin	WA			1999-MM-DD	*Medicago sativa*
	Moulamein	NSW	–35.09	144.04	2022-10-04	Mixed pasture

Table 2. Results from insecticide bioassays on transgenic *Drosophila melanogaster* carrying our candidate E4-like esterase from *Acyrthosiphon kondoi*. Reported are the intercepts (b_0), slopes (b_1), χ^2 goodness-of-fit statistics and associated *P*-values, LD_{50} values (mg a.i./L) with 95% confidence intervals, and resistance ratios (RR) of mutant strains. (See also Figure 4)

Insecticide	**Strain**	b_0	b_1	χ^2 **(df)**	$P(\chi^2)$	**LD50 values (95% CIs)**	**RR**
Alpha-cypermethrin	Control	0.32	4.15	0.4 (3)	0.94	0.84 (0.74,0.94)	
	Mutant	–2.09	3.76	0.65 (3)	0.88	3.6 (3.16,4.11)	4.31
Chlorpyrifos	Control	4.06	3.67	0.51 (3)	0.92	0.08 (0.07,0.09)	
	Mutant	1.79	4.39	0.41 (3)	0.94	0.39 (0.36,0.43)	4.99
Pirimicarb	Control	–8.64	4.09	0.4 (3)	0.94	130.5 (118.01,144.31)	
	Mutant	–10.61	4.05	0.6 (3)	0.90	416.7 (369.71,469.66)	3.19

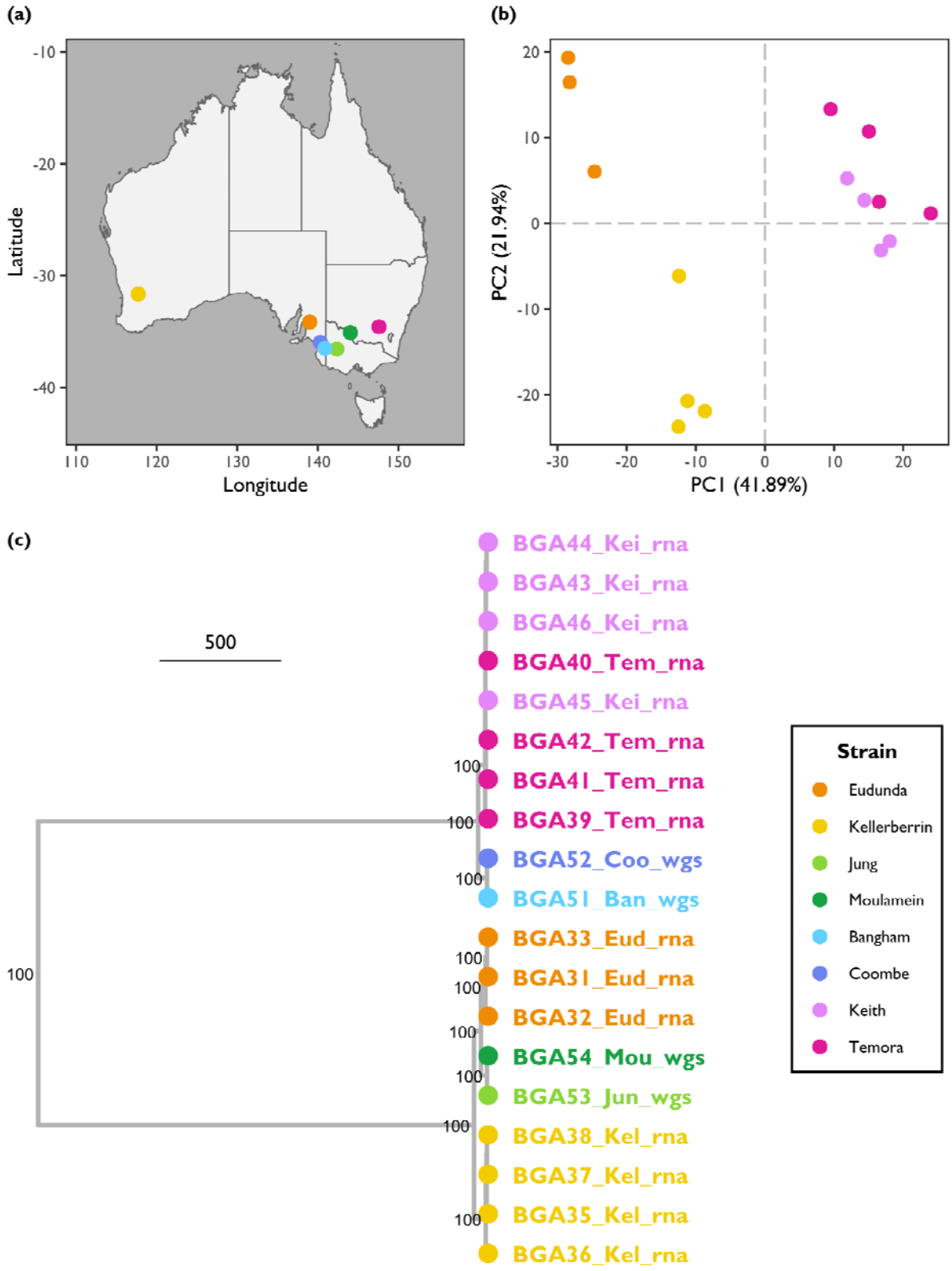

Figure 1. Transcriptomic and genetic comparisons of *Acyrthosiphon kondoi* strains examined in this study. The susceptible strains include Eudunda (Eud), Kellerberrin

(Kel), Jung (Jun) and Moulamein (Mou). The resistance strains include Bangham (Ban), Coombe (Coo), Keith (Kei) and Temora (Tem). (a) Source locations of each strain in Australia: note, Keith and Coombe overlap in the map. (b) Transcriptomic profiles of the Eudunda, Kellerberrin, Keith and Temora strains projected into principal component space. Percentages in parentheses on the x-axis and y-axis capture the amount of variance explained by the first and second PC axis, respectively. (c) A UPGMA tree constructed from allelic distances among samples of each strain. Branch nodes are labelled with bootstrap values >80%. Samples follow the naming convention 'ID_Strain_Method', where 'ID' is a unique sample identifier, 'Strain' is one of the eight sampled strains, and 'Method' is one of 'rna' for transcriptome sequencing or 'wgs' for whole-genome sequencing. (a–c) Points are coloured by strain, see the legend.

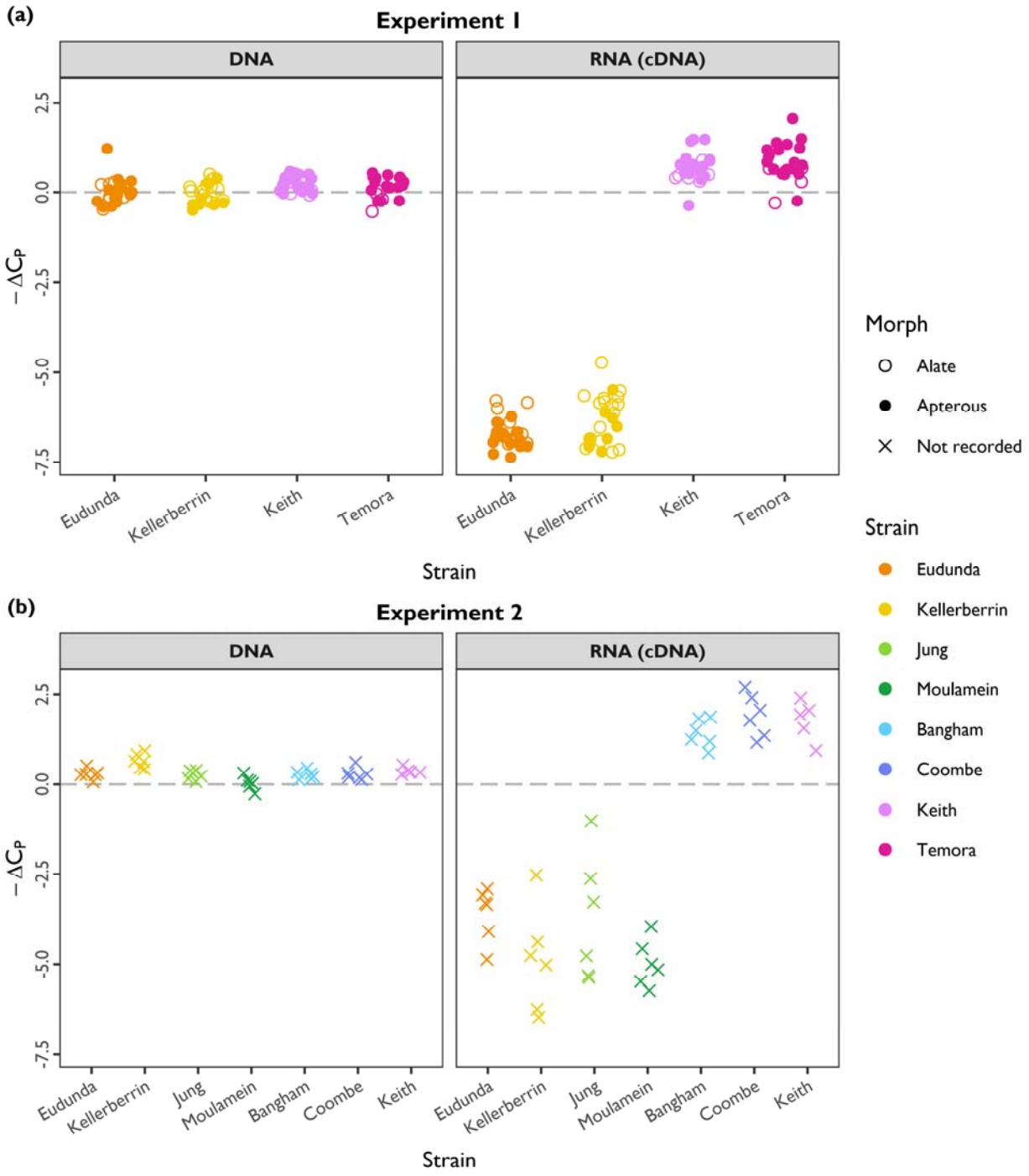

Figure 2. Among-strain comparisons of candidate E4-like esterase relative genomic copy number and expression in 12-day-old *Acyrthosiphon kondoi* measured with qPCR. Clonal strains are arranged on the x-axis. The $-\Delta C_P$ is on the y-axis, which represents the inverse of the ΔC_P, where the ΔC_P = E4-like esterase C_P – actin C_P. A

positive $-\Delta C_P$ therefore indicates a higher amplification of the E4-like esterase (more molecules), and a negative $-\Delta C_P$ indicates a lower amplification of the E4-like esterase (fewer molecules), relative to the reference actin gene. Panels contain results from DNA samples (left) and RNA/cDNA samples (right). The dashed grey line demarcates a $-\Delta C_P$ of 0, that is, no difference in the amplification of the E4-like esterase and actin genes. Points are coloured by strain, with shapes indicating the aphid morph (see legend). (a) Experiment 1: individual-level measurements for the original four strains (Eudunda, Kellerberrin, Keith and Temora) and between alate versus apterous morphs. (b) Experiment 2: pooled measurements (two aphids per sample) for the additional strains (Jung, Moulamein, Bangham and Coombe) with the original susceptible strains (Eudunda and Kellerberrin) and a resistant strain (Keith) used as a comparison.

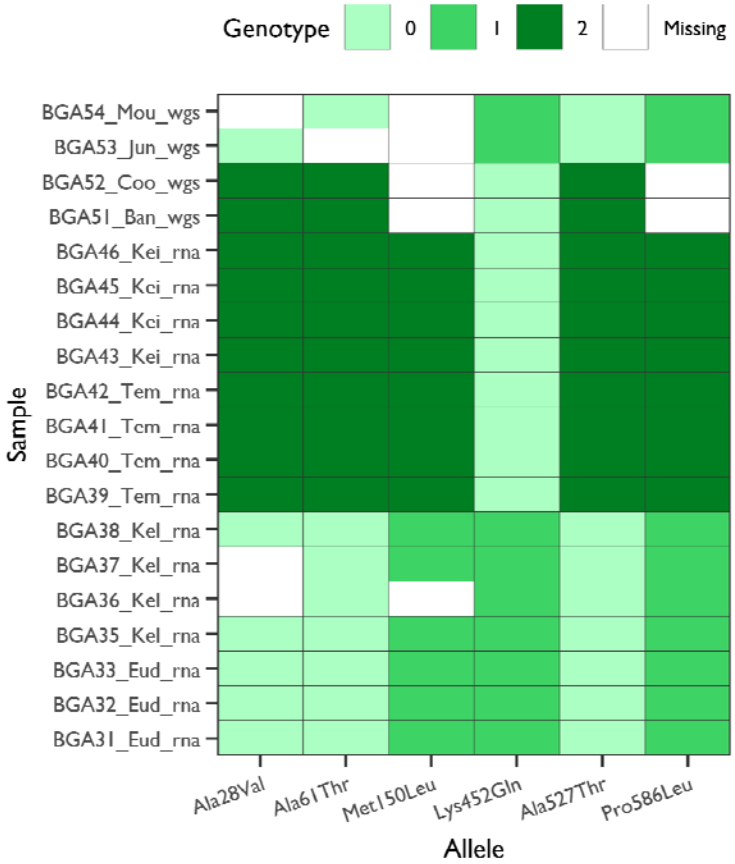

Figure 3. Non-synonymous mutations in the candidate E4-like esterase gene annotated in the genome of *Acyrthosiphon kondoi*. Mutant alleles are arranged along the *x*-axis. Samples are arranged on the *y*-axis, labelled as 'ID_Strain_Method', where 'ID' is a unique sample identifier, 'Strain' is one of the eight clonal strains, and 'Method' is one of 'rna' for transcriptome sequencing or 'wgs' for whole-genome sequencing. Cell colours indicate the observed genotype (see legend). The susceptible strains include Eudunda (Eud), Kellerberrin (Kel), Jung (Jun) and Moulamein (Mou). The resistance strains include Bangham (Ban), Coombe (Coo), Keith (Kei) and Temora (Tem).

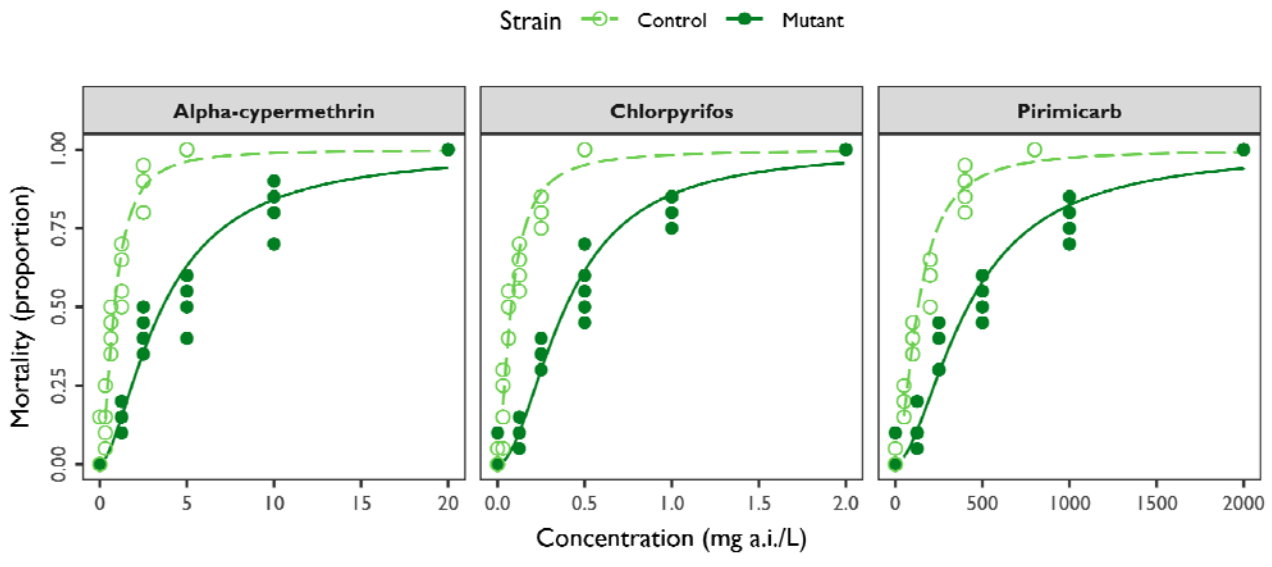

Figure 4. Dose-responses generated from insecticide bioassays on transgenic *Drosophila melanogaster* carrying our candidate E4-like esterase from *Acythosiphon kondoi*. The *x*-axis represents the concentration of insecticide, and the *y*-axis represents the proportion of mortality. Points represent individual replicates with predicted dose response curves (line type and colour depicts strains, see legend). Panels contain data for different insecticides tested (see also Table 2).

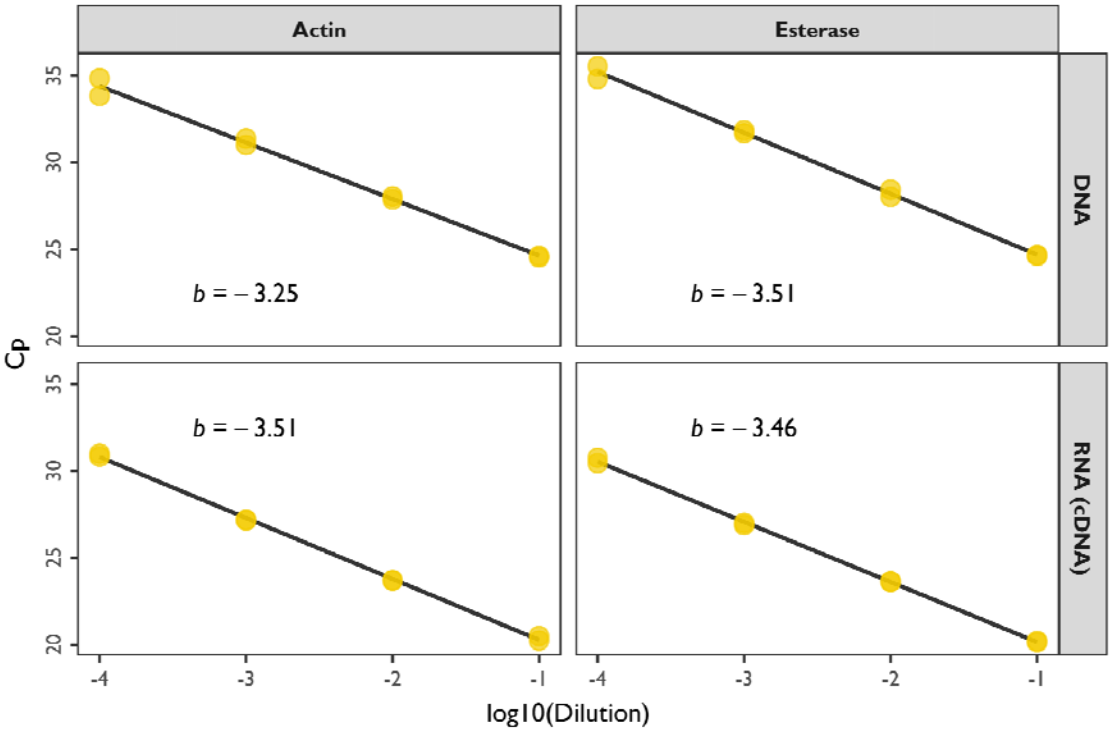

Figure S1. Primer efficiency test for estimating relative expression of the E4-like esterase. The *x*-axis represents the log10-transformed dilution factor of nucleic acid, whereas the *y*-axis represents the mean Cp value obtained in qPCR. Points represent different samples. Black lines indicate the line of best fit. The slope of the line, *b*, is also labelled on the plots: values between −3.3 and −3.6 are good. Panels separate results for the nucleic acid origin (in rows: DNA or RNA) and gene (in columns: actin or the esterase). These efficiency tests were performed on extractions prepared from the Kellerberrin strain.

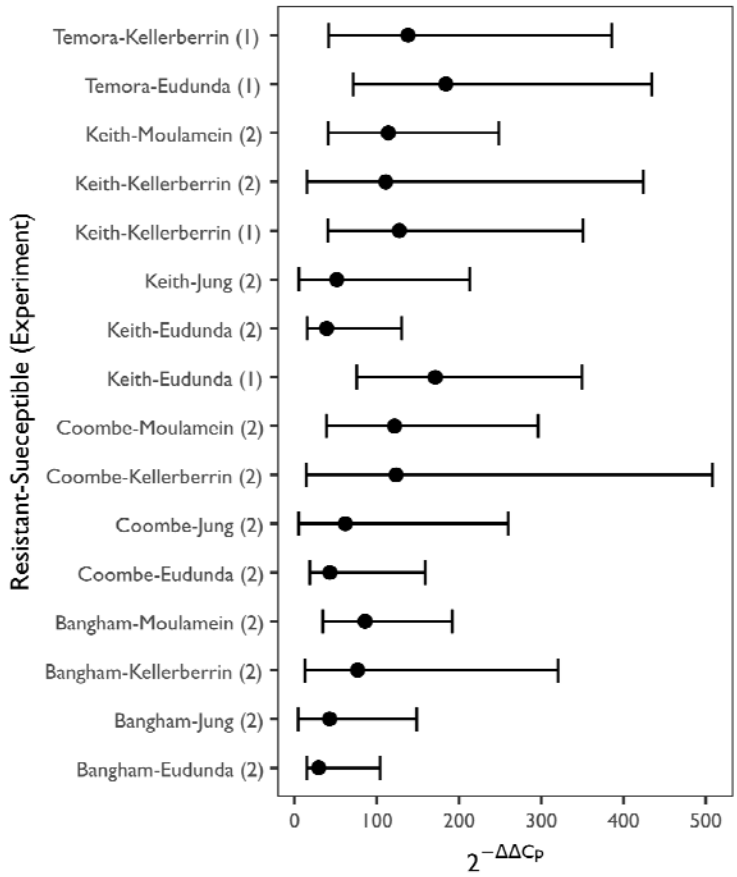

Figure S2. E4-like esterase fold-change expression differences between resistant vs. susceptible strains of *Acyrthosiphon kondoi*. The *x*-axis represents the measured fold-change difference, and the *y*-axis represents comparisons between different strains. Labels on the *y*-axis are presented as resistant vs susceptible with experimental number in parentheses. Points indicate median estimates of fold-change expression differences, with error bars indicating the 2.5% and 97.5% confidence intervals.

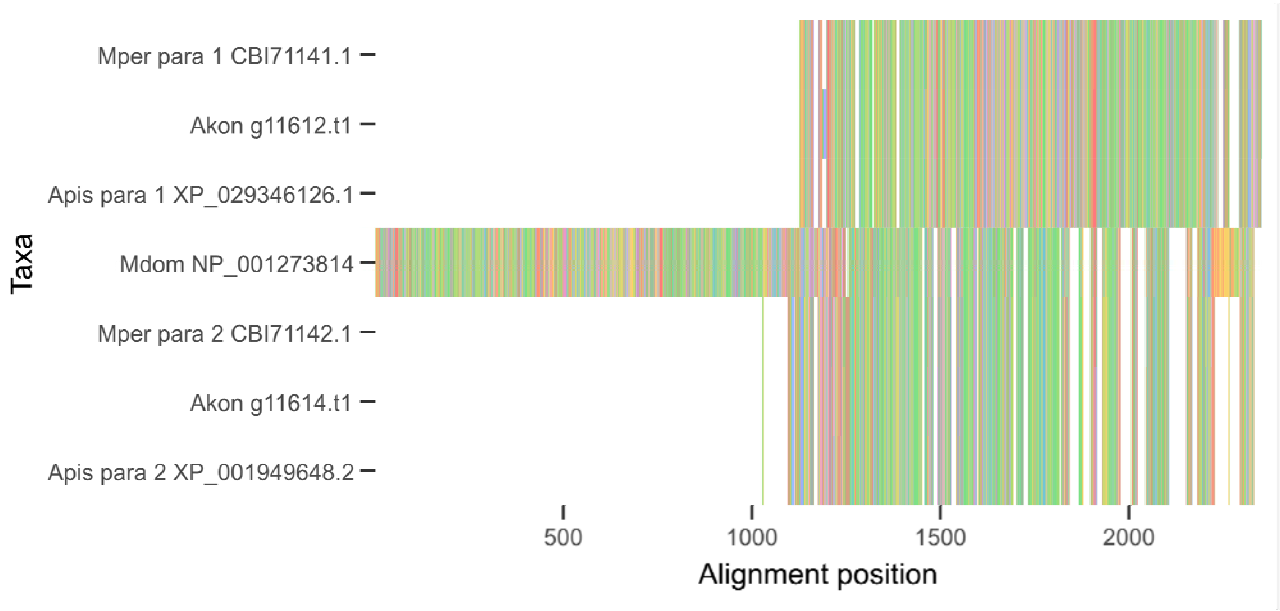

Figure S3. Alignment of *Acrythosiphon kondoi* (Akon) annotated *para* proteins to the canonical reference sequence, *Musca domestica* (Mdom), and to subunit 1 and 2 sequences found in the aphids *Myzus persicae* (Mper) and *A. pisum* (Apis). The alignment position is on the *x*-axis with species arranged on the *y*-axis.

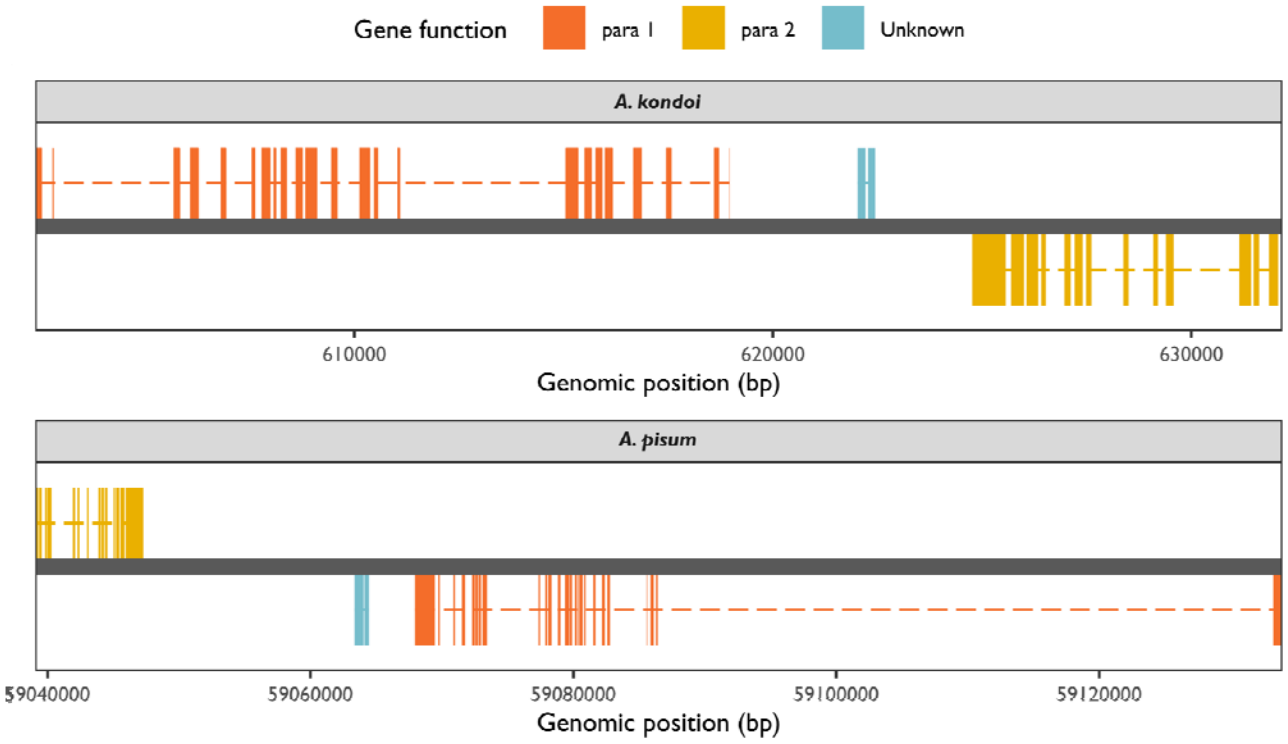

Figure S4. Genomic regions containing *para* genes in our reference assembly of *Acyrthosiphon kondoi* and in the reference assembly of *A. pisum* (NCBI Genome Accession GCF_005508785.1). The *x*-axis represents the genomic position in base pairs. The dark grey horizontal bar represents the genome. Coloured bars represent the exons of different genes, those on top represent genes on the positive strand, whereas those on the bottom represent genes on the negative strand. Dashed lines connect exons within the same gene. Exons are coloured by their gene function (see legend).

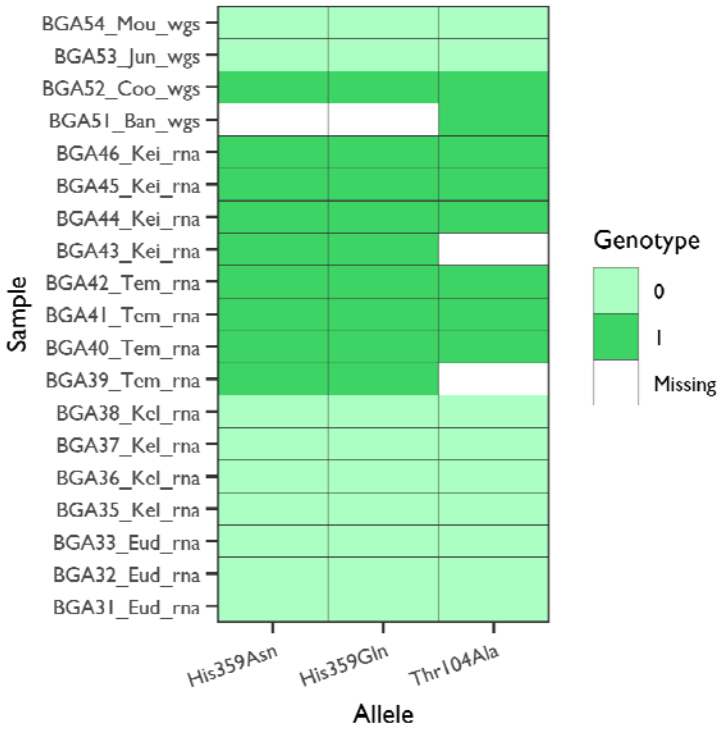

Figure S5. Non-synonymous mutations in the *para* g11614 gene annotated in the genome of *Acyrthosiphon kondoi*. Mutant alleles are arranged along the *x*-axis. Samples are arranged on the *y*-axis, labelled as 'ID_Strain_Method', where 'ID' is a unique sample identifier, 'Strain' is one of the eight clonal strains, and 'Method' is one of 'rna' for transcriptome sequencing or 'wgs' for whole-genome sequencing. Cell colours indicate the observed genotype (see legend). The susceptible strains include Eudunda (Eud), Kellerberrin (Kel), Jung (Jun) and Moulamein (Mou). The resistance strains include Bangham (Ban), Coombe (Coo), Keith (Kei) and Temora (Tem).

Table S1. Mortality of different *Acyrthosiphon kondoi* isofemale clonal strains to a water control and treatment of 15 mg a.i./L of chlorpyrifos in a leaf dip bioassay (72 hours exposure).

Status	Strain	mg/L	Replicates	Aphids	Mean	CI 2.5%	CI 97.5%
Resistant	Bangham	0	6	30	0		
		15	6	30	0.333	0.19	0.516
	Coombe	0	6	30	0		
		15	6	30	0.433	0.271	0.612
	Keith	0	6	30	0		
		15	10	50	0.04	0.01	0.146
	Temora	0	6	30	0		
		15	10	50	0.06	0.019	0.17
Susceptible	Eudunda	0	6	30	0.033	0.005	0.202
		15	10	50	1		
	Jung	0	6	30	0		
		15	6	30	1		
	Kellerberrin	0	6	30	0		
		15	10	50	1		
	Moulamein	0	6	30	0		
		15	6	30	1		

Table S2. Significantly over-expressed genes found in all four pairwise combinations of resistance (Keith and Temora) vs. susceptible (Kellerberrin and Eudunda) strains.

Gene ID	Function	Mean fold-change	Mean *p*-value	Mean rank	GO terms
g15286	esterase E4-like	201.7	7.8e–268	1	GO:0080030
g8122	voltage-dependent anion-selective channel-like isoform X2	107.0	8.0e–244	2	GO:0005741 GO:0046930 GO:0000166 GO:0008308 GO:0015288 GO:0015698 GO:0098656 GO:1902017
g17538	mutS protein homolog 4-like	79.4	2.5e–137	4	GO:0005524 GO:0016787 GO:0030983 GO:0140664 GO:0006298
g7800		43.1	1.8e–107	4	
g7378	Pogo transposable element with KRAB domain	287.1	7.8e–104	6	GO:0003676
g16956	uncharacterized protein LOC103310965	711.7	5.7e–79	7	GO:0042575 GO:0003676 GO:0003887 GO:0015074 GO:0071897
g13864	putative sodium-dependent multivitamin transporter	15.9	8.1e–100	8	GO:0016020 GO:0022857

					GO:0055085
g20808	zinc finger CCHC domain-containing protein 10-like	13.9	2.0e–64	8	GO:0003676 GO:0008270
g8121		48.7	1.5e–79	9	
g690	cactin	23.7	6.1e–58	11	
g338	microtubule-associated protein Jupiter-like isoform X2	55.1	5.3e–78	12	GO:0005634 GO:0005737 GO:0005819 GO:0005874
g20001	Integrase catalytic domain-containing protein	165.9	6.5e–72	12	GO:0042575 GO:0003676 GO:0003887 GO:0015074 GO:0071897
g11905	uncharacterized protein LOC115034590	9.7	3.7e–57	13	
g11752	CCHC-type domain-containing protein	33.2	7.1e–42	13	
g6025	Integrase catalytic domain-containing protein	72.4	7.6e–45	18	GO:0042575 GO:0003676 GO:0003887 GO:0015074 GO:0071897
g18489	semaphorin-1A-like	4.8	4.9e–39	20	GO:0016020 GO:0030215 GO:0007399 GO:0030154
g18463	ATP-binding cassette sub-family B member 7, mitochondrial	4.1	9.2e–38	20	GO:0016020 GO:0043229 GO:0005524 GO:0016279 GO:0140359

					GO:0018023 GO:0055085
g13749	protein toll-like	4.8	1.9e–49	21	GO:0002224 GO:0004888 GO:0016020
g19161	protein scarlet	5.3	8.0e–35	21	GO:0016020 GO:0005524 GO:0016787 GO:0140359 GO:0055085
g19170	aurora kinase C	14.7	5.5e–35	25	GO:0004674 GO:0005524 GO:0006468
g4041	MULE domain-containing protein	4.4	8.5e–32	25	
g86	Endonuclease/exonuclease/phosphatase,Reverse transcriptase domain	15.7	2.4e–38	28	GO:0003964 GO:0004519 GO:0004527 GO:0006278 GO:0090305
g15498	trafficking protein particle complex subunit 3	4.8	1.3e–28	31	GO:0005783 GO:0005794 GO:0030008 GO:0048193
g22102	MULE domain-containing protein	7087.0	1.2e–29	32	
g25847	caspase-1-like	8.3	2.1e–33	35	GO:0004197 GO:0006508 GO:0042981
g3625	uncharacterized protein LOC111042072	9.6	2.2e–20	36	GO:0071897
g10009	zinc finger MYM-type protein 1-like isoform X1	36.0	9.4e–26	37	

g13578	putative serine protease K12H4.7	1943.5	6.8e–24	44	GO:0008236 GO:0006508
g11384	coiled-coil domain-containing protein 1-like isoform X1	13.5	2.4e–16	46	GO:0003677 GO:0003950
g17096	CUGBP Elav-like family member 4 isoform X1	26770.4	1.6e–25	48	GO:0003723
g7323	Integrase catalytic domain-containing protein	758.1	1.4e–26	50	GO:0005488 GO:0006259
g5654	general transcription factor II-I repeat domain-containing protein 2-like	891.2	9.6e–22	50	GO:0006259
g7941	Macro domain-containing protein	3.9	1.5e–17	53	GO:0003676 GO:0008270
g8123	COP9 signalosome complex subunit 4	6.5	1.7e–13	53	GO:0000502 GO:0005576 GO:0005737 GO:0008180 GO:0003677 GO:0004672 GO:0005524 GO:0006468
g14356	U3 small nucleolar RNA-associated protein 6 homolog	4.6	2.7e–14	54	GO:0005634 GO:0030515 GO:0000462
g20598	histone H1A, sperm-like	3.2	6.5e–18	55	GO:0000786 GO:0005634 GO:0003677 GO:0030527 GO:0006334
g16957	Integrase catalytic domain-containing protein	3648.9	5.3e–22	56	GO:0042575 GO:0003676 GO:0003887

					GO:0015074 GO:0071897
g24560	RNA-directed DNA polymerase from mobile element jockey	3.1	1.3e–17	58	GO:0004518 GO:0071897
g22560	Integrase catalytic domain-containing protein	23.9	6.6e–20	59	GO:0042575 GO:0003676 GO:0003887 GO:0015074 GO:0071897
g11751	putative cytochrome P450 6a14	12.9	9.6e–13	59	GO:0003824 GO:0071897
g25054	E3 SUMO-protein ligase ZBED1-like	1835.8	1.7e–20	61	GO:0005488
g13338	kinesin-like protein KIF21A isoform X1	5.7	3.6e–16	61	GO:0000166 GO:0003774
g15285	cytochrome P450 6k1 isoform X2	6.3	9.7e–16	61	GO:0016020 GO:0004497 GO:0005506 GO:0016705 GO:0020037
g8215	DUF4806 domain-containing protein	2513.8	2.1e–21	63	
g25387	RING-type domain-containing protein	617.9	4.8e–18	65	
g3626	uncharacterized protein LOC126553589, partial	8.7	8.7e–17	65	GO:0042575 GO:0000166 GO:0003677 GO:0003887 GO:0006260 GO:0071897
g689	ring canal kelch homolog isoform X2	3.9	9.9e–10	65	GO:0005622
g10656	probable G-protein coupled receptor Mth-like 3 isoform X1	5.9	2.5e–19	67	GO:0005886 GO:0004930

					GO:0007166 GO:0007186
g16885	uncharacterized protein LOC111028208	5368.7	1.3e–17	71	
g22575	C2H2-type domain-containing protein	123.0	2.6e–19	73	
g19948	phosphatidylserine synthase 1	2.7	1.2e–17	75	GO:0005789 GO:0106245 GO:0006098 GO:0006119 GO:0006526 GO:0006659 GO:0015012 GO:0015940
g25969	Integrase, catalytic core,Ribonuclease H-like domain,Macro domain	1261.8	1.4e–17	76	GO:0016020 GO:0016779 GO:0006259
g2017	UDP-glycosyltransferase UGT5-like	3.6	9.5e–17	76	GO:0016020 GO:0015020
g22423	nucleoporin NUP53 isoform X1	2.0	9.6e–16	81	GO:0005643 GO:0031965 GO:0003676 GO:0017056 GO:0006913 GO:0015031 GO:0051028
g1150	DUF1298 domain-containing protein	2.6	7.9e–11	81	GO:0016020 GO:0004144 GO:0045017
g5923	Uncharacterized protein FWK35_00014710	1138.0	7.8e–17	82	
g23115	SWIM-type domain-containing protein	162.3	4.3e–16	82	
g5605	uncharacterized protein LOC103311701	31.5	7.8e–17	83	GO:0042575

					GO:0003676 GO:0003887 GO:0015074 GO:0071897
g2226	proteasome subunit beta type-like	2.3	1.0e–10	85	GO:0005634 GO:0005839 GO:0016787 GO:0010498
g28211	ATP-dependent DNA helicase	5.3	4.1e–15	86	GO:0016740
g15029	E3 ubiquitin-protein ligase RNF8-like isoform X2	5.9	4.6e–10	88	
g27754	ring canal kelch homolog isoform X2	2996.3	7.2e–16	91	
g24378	MULE domain-containing protein	4.9	4.8e–13	92	
g3627	zinc finger protein 668-like	10.3	1.0e–14	97	GO:0016740
g24738	uncharacterized protein K02A2.6-like	2522.4	5.9e–15	98	
g4646	piggyBac transposable element-derived protein 4-like	4.6	2.1e–13	98	GO:0016020 GO:0008270
g13843	SET and MYND domain-containing protein 4	2.5	1.2e–08	98	GO:0005634 GO:0046872
g23325	Transposon Ty3-I Gag-Pol polyprotein	2570.7	2.2e–15	99	GO:0016779 GO:0006259
g26123	ring canal kelch homolog	97.0	5.2e–14	100	GO:0003779 GO:0016567
g5435	T-complex protein 1 subunit alpha	6.1	1.4e–14	102	GO:0005524 GO:0016887 GO:0051082 GO:0140662 GO:0006457
g5843	Uncharacterized protein FWK35_00030346,	4.7	2.4e–08	102	

	partial				
g22412	60S ribosomal protein L12	2.0	1.8e–10	105	GO:0005840 GO:1990904 GO:0003735 GO:0006412
g9376	RNA-binding protein 42-like isoform X1	2.4	1.1e–08	109	GO:0003723
g21759	kelch-like protein 3 isoform X3	23.3	9.6e–15	110	
g10330	Uncharacterized protein FWK35_00036217	52.6	2.1e–12	110	GO:0003676 GO:0003824 GO:0008270
g16823	DUF4806 domain-containing protein	2221.9	4.7e–14	111	
g23014	hypothetical protein AGLY_012350	1857.3	9.5e–14	111	
g19196	AP2/ERF domain-containing protein PFD0985w-like	97.4	2.1e–09	111	GO:0042575 GO:0003676 GO:0003887 GO:0003964 GO:0004190 GO:0006278 GO:0006508 GO:0015074
g13698	kinesin-related protein 2-like	7.7	2.3e–08	111	GO:0003677 GO:0004803 GO:0006313
g25058	ribosomal protein L22	1876.5	1.1e–13	112	GO:0005840 GO:1990904 GO:0003735 GO:0006412
g10894	ADP-ribose glycohydrolase OARD1-like	106.5	1.3e–07	113	
g2679	ARL14 effector protein-like	2.3	6.8e–08	114	
g24945	Integrase catalytic domain-containing	2098.8	6.9e–13	115	GO:0042575

	protein				GO:0003676 GO:0003887 GO:0015074 GO:0071897
g3921	uncharacterized protein LOC111041156	21.2	1.8e–10	115	
g23012	tigger transposable element-derived protein 7-like	1650.7	5.1e–13	117	GO:0003677
g21514	ACYPI45661	2.1	4.8e–11	117	
g23444	Reverse transcriptase domain	1750.2	5.9e–13	118	GO:0016020 GO:0003824 GO:0071897
g2552	kinetochore protein NDC80 homolog	2.5	3.8e–06	118	GO:0005634 GO:0031262 GO:0051301 GO:0051315
g5962	Reverse transcriptase domain	1637.6	1.1e–13	122	GO:0016020 GO:0004518 GO:0071897
g25317	Jerky-like	1558.2	6.3e–13	123	GO:0003677
g21472	ring canal kelch homolog isoform X1	4.6	1.5e–10	123	GO:0005737 GO:0016020 GO:0004721 GO:0016311 GO:0036211 GO:0048856
g8480	1-acyl-sn-glycerol-3-phosphate acyltransferase gamma-like	10.3	1.3e–08	124	GO:0016020 GO:0016746
g22126	zinc finger MYM-type protein 1-like	1589.4	8.9e–13	125	GO:0046983
g24377	MULE domain-containing protein	6.9	2.9e–09	127	
g27938	uncharacterized protein LOC111028208	1545.4	6.6e–13	128	

g8235	putative nuclease HARBI1	190.9	1.2e–13	131	GO:0005634 GO:0016787 GO:0046872
g12560	interaptin-like isoform X1	3.2	1.9e–05	131	
g1264	beta-chimaerin isoform X1	2.0	3.1e–06	135	GO:0016301 GO:0007165 GO:0016310
g14292	UDP-glucuronosyltransferase 2B20	2.7	2.6e–08	139	GO:0016020 GO:0015020
g3933	MULE domain-containing protein	3.0	5.1e–06	140	
g2824	THAP-type domain-containing protein	1201.8	1.7e–12	141	GO:0005654 GO:0004803 GO:0043565 GO:0046872 GO:0006313 GO:0007049
g14181	heparanase-like	2.3	2.2e–06	145	GO:0016020 GO:0016798
g26944	Transposon Ty3-I Gag-Pol polyprotein	1163.0	2.9e–12	146	GO:0003676 GO:0004190 GO:0008270 GO:0140097 GO:0006508 GO:0071897
g15628	transposase	193.1	1.3e–11	146	GO:0006259
g4033	adenylate kinase isoenzyme 6	1.9	1.4e–11	146	GO:0005634 GO:0004017 GO:0005524 GO:0016887 GO:0016310

					GO:0046940
g14481	leucine-rich repeat-containing protein 59-like	2.3	1.1e–10	148	GO:0016020
g1649	tubulointerstitial nephritis antigen-like	7.4	1.5e–08	148	
g21539	balbiani ring protein 3	2.2	6.8e–07	151	
g25899	DNA polymerase epsilon subunit 2	2.1	1.2e–06	152	GO:0008622 GO:0003677 GO:0006261
g23013	jerky protein homolog-like	970.8	1.5e–11	155	GO:0003677
g5340	52 kDa repressor of the inhibitor of the protein kinase-like	977.1	1.3e–11	158	GO:0005488
g12559	bifunctional 3'-5' exonuclease/ATP-dependent helicase WRN-like	2.4	5.4e–06	158	GO:0005634 GO:0003676 GO:0005524 GO:0016887 GO:0043138 GO:0006260 GO:0006281 GO:0006310 GO:0032508
g17842	zinc finger MYM-type protein 1-like	6.3	6.1e–08	161	
g21028	macrophage erythroblast attacher	2.5	3.0e–06	162	GO:0005737 GO:0016363 GO:0046872 GO:0061630 GO:0016567 GO:0043161 GO:0043249
g13845		3.1	2.7e–08	164	
g16459	FACT complex subunit Ssrp1	2.9	8.2e–10	165	GO:0005634

					GO:0005694 GO:0003677 GO:0006260 GO:0006281 GO:0016043
g24343	F-box/WD repeat-containing protein 7 isoform X2	8.1	2.3e–08	166	
g21630	RNA-binding protein 42-like isoform X1	2.6	1.0e–06	166	GO:0003723
g13693	lymphoid-specific helicase	2.5	2.6e–09	170	GO:0016020 GO:0043229 GO:0004386 GO:0005524 GO:0140658 GO:0006338
g23324	Transposon Ty3-I Gag-Pol polyprotein	869.8	5.5e–11	171	GO:0016779 GO:0006259
g5483	zinc finger BED domain-containing protein RICESLEEPER 1-like isoform X1	855.4	4.3e–10	172	GO:0046983
g17138	outer dense fiber protein 3-like protein 2	7.3	1.0e–09	173	
g15561	DUF4806 domain-containing protein	5.0	5.3e–06	174	
g7399	ADP-ribosylation factor 2	2.7	5.6e–07	177	GO:0005794 GO:0003924 GO:0005525 GO:0015031 GO:0016192 GO:0048731 GO:0051649
g6034	heat shock protein cognate 3 precursor	12.1	7.1e–09	180	GO:0005788 GO:0005524 GO:0140662

					GO:0006457
g1752	pterin-4-alpha-carbinolamine dehydratase-like	1.7	6.2e–09	184	GO:0008124 GO:0006729
g16107	zinc finger MYM-type protein 1-like	231.5	1.9e–04	186	GO:0046983
g6298	UDP-glucuronosyltransferase 2B15	4.5	1.3e–03	186	GO:0016020 GO:0015020
g11774	1,5-anhydro-D-fructose reductase	1.9	2.7e–06	188	GO:0016491
g16038	HTH CENPB-type domain-containing protein	645.6	4.3e–10	189	
g252	Transposon Ty3-I Gag-Pol polyprotein	6.6	3.1e–09	190	GO:0005488 GO:0016787 GO:0034061 GO:0071897
g3935	RING finger protein 17 isoform X1	2.0	1.7e–07	191	
g11328	MULE domain-containing protein	2.9	3.8e–05	193	
g22112	ACYPI24120 protein	591.2	2.6e–09	196	
g3936	tudor domain-containing protein 1-like	2.6	1.3e–04	196	
g15100	Endonuclease/exonuclease/phosphatase,Reverse transcriptase domain	765.3	2.5e–09	198	GO:0090304
g11432	phosphoinositide 3-kinase regulatory subunit 4	2.2	1.3e–03	201	GO:0016020 GO:0004674 GO:0005524 GO:0006468 GO:0016236 GO:0045324
g7413	peptide transporter family 1 isoform X1	2.9	1.1e–04	202	GO:0016020 GO:0022857 GO:0006857 GO:0055085
g2120	ring canal kelch homolog	9.1	3.4e–04	204	

g7494	nuclear pore complex protein Nup160-like	22.6	8.3e–07	205	GO:0005643 GO:0003676 GO:0006913 GO:0033036 GO:0043170 GO:0071702 GO:0071705
g24858		563.6	1.4e–09	210	
g3628	uncharacterized protein LOC103308809	8.1	2.2e–06	210	GO:0004623 GO:0005198 GO:0006644 GO:0050482
g21982	MULE domain-containing protein	539.5	2.6e–09	211	
g28248	SWIM-type domain-containing protein	585.4	1.5e–08	215	
g9657	Myb/SANT-like transcription factor	5.1	1.3e–04	216	
g22800	aldehyde dehydrogenase, mitochondrial-like isoform X1	2.3	1.0e–03	219	GO:0016620
g24615	7TM chemoreceptor	82.2	1.3e–07	220	GO:0016020
g19520	GPALPP motifs-containing protein 1	1.6	2.6e–08	221	GO:0044238 GO:0071704
g3629	general transcription factor II-I repeat domain-containing protein 2-like	15.6	2.5e–06	221	GO:0003677 GO:0004803 GO:0006313
g24217	tigger transposable element-derived protein 6-like	513.5	1.5e–08	225	GO:0005634 GO:0003677
g14187	Bromodomain	2.5	1.3e–04	226	
g11229	RYamide receptor-like	2.1	4.0e–07	229	GO:0016020 GO:0004983 GO:0007218

g14316	ACYPI003107	2.1	8.2e–05	229	
g17194	SWIM-type domain-containing protein	494.6	4.9e–09	235	GO:0008270
g1913	cysteine and histidine-rich domain-containing protein	3.4	8.4e–05	235	GO:0046872
g25087	RING-type domain-containing protein	457.4	6.1e–09	237	
g24452	GTPase Era, mitochondrial-like	1.6	2.3e–04	237	GO:0003723 GO:0005525
g18354	lipid droplet-associated hydrolase	2.0	2.6e–04	237	GO:0005811 GO:0016020 GO:0016298 GO:0019915
g22114	Lebercilin domain-containing protein	445.5	1.1e–08	238	
g6364	insulin-like growth factor-binding protein-related protein 1	1.8	2.2e–04	241	GO:0005576 GO:0005520 GO:0001558
g8202	protein ALP1-like	495.0	8.6e–09	242	GO:0005634 GO:0016787 GO:0046872
g20212	THAP-type domain-containing protein	2.3	1.1e–04	242	GO:0003677 GO:0004803 GO:0008270 GO:0006313
g26357	Hypothetical predicted protein	2.3	6.3e–07	243	GO:0016020
g2545	asparagine--tRNA ligase, cytoplasmic	1.5	1.5e–05	243	GO:0003676 GO:0004816 GO:0005524 GO:0006421
g11366		2.5	4.7e–04	243	
g14021	DNA topoisomerase 2-binding protein 1	1.7	5.5e–04	250	GO:0016853

	isoform X3				
g6544		2.1	9.3e–04	250	
g9254	MULE domain-containing protein	29.3	3.5e–05	254	
g25230	putative nuclease HARBI1	410.3	1.6e–08	257	
g10550	Kinesin-like protein unc-104	34.3	2.3e–06	257	
g18444	zinc finger protein OZF-like	2.9	1.4e–04	264	
g23157	Transposon Ty3-G Gag-Pol polyprotein	139.7	9.4e–08	269	GO:0003824 GO:0071897
g11365		2.9	1.4e–04	269	
g25800	Haemolymph juvenile hormone binding	2.2	4.0e–06	270	
g9297	GTP-binding protein REM 1-like isoform X2	2.1	5.2e–06	275	GO:0003924 GO:0005525
g1136	plexin-B-like	3.7	9.0e–04	284	
g14842	queuine tRNA-ribosyltransferase accessory subunit 2-like	1.9	1.4e–03	289	GO:0005737 GO:0008479 GO:0046872 GO:0101030
g15294	unnamed protein product	115.5	3.4e–06	290	GO:0071897
g11227		5.9	6.2e–05	293	
g2799	serpin B4 isoform X1	2.2	3.1e–06	295	GO:0005615 GO:0016020 GO:0004867 GO:0010951
g4580	facilitated trehalose transporter Tret1 isoform X3	2.0	6.2e–04	297	GO:0016020 GO:0022857 GO:0055085
g4144	uncharacterized protein LOC115034986	303.5	6.7e–07	303	
g9607	serpin B4 isoform X1	1.7	1.1e–05	313	GO:0005615

					GO:0016020 GO:0004867 GO:0010951
g6306	NAD-dependent protein deacetylase Sir2B-like	114.3	5.7e–06	314	
g23948	activating signal cointegrator 1 complex subunit 2-like	11.8	1.3e–03	316	GO:0043130
g23872	ACYPI004125	1.6	1.6e–04	317	GO:0005783 GO:0005509 GO:0030246 GO:0051082 GO:0006457
g313	Myb DNA-bind 2 domain-containing protein	2.3	9.5e–04	324	GO:0000781 GO:0005634 GO:0016020 GO:0006355 GO:0010833
g7503	cystathionine beta-synthase isoform X3	27.5	3.2e–06	328	GO:0005737 GO:0004122 GO:0006535 GO:0019343
g26218	Reverse transcriptase domain	4.2	9.3e–05	329	GO:0003964 GO:0004519 GO:0004527 GO:0006278 GO:0090305
g26788	mitochondrial import inner membrane translocase subunit Tim22	1.6	6.5e–04	331	GO:0042721 GO:0008320 GO:0045039 GO:0071806
g15281	DUF4806 domain-containing protein	16.0	1.1e–03	332	

g4848	epimerase family protein SDR39U1-like	1.5	1.4e–03	339	GO:0004672 GO:0005524 GO:0006468
g1629	farnesol dehydrogenase-like	1.5	1.1e–03	366	
g4487	eukaryotic translation initiation factor eIF1	1.6	1.3e–03	366	GO:0003743 GO:0006413
g13825		1.6	2.5e–03	368	
g17321	retrovirus-related Pol polyprotein from type-2 retrotransposable element R2DM	1.6	2.1e–03	369	GO:0009536 GO:0003824 GO:0005488 GO:0071897
g9603	leukocyte elastase inhibitor	2.5	1.3e–04	373	GO:0005615 GO:0004867 GO:0010951
g4462	ACYPI53166	2.2	1.8e–03	421	GO:0016020

Table S3. Fold-change difference in the expression of the candidate E4-like esterase between resistant and susceptible strains estimated from qPCR assays with the $2^{-\Delta\Delta C_P}$ method. Median values with 2.5% and 97.5% percentiles for the estimates are reported.

Experiment	Resistant	Susceptible	Median	2.5%	97.5%
1	Keith	Eudunda	171	76	350
	Keith	Kellerberrin	128	41	351
	Temora	Eudunda	184	71	434
	Temora	Kellerberrin	138	42	386
2	Bangham	Eudunda	29	15	104
	Bangham	Jung	43	5	149
	Bangham	Kellerberrin	77	13	321
	Bangham	Moulamein	86	34	192
	Coombe	Eudunda	43	19	159
	Coombe	Jung	62	5	260
	Coombe	Kellerberrin	124	15	508
	Coombe	Moulamein	122	39	296
	Keith	Eudunda	39	16	130
	Keith	Jung	52	5	213
	Keith	Kellerberrin	111	15	424
	Keith	Moulamein	114	41	249